#202

FACILITY FORM 602

N65-85776	
(ACCESSION NUMBER)	(THRU)
44	None
(PAGES)	(CODE)
CR 63454	
(NASA CR OR TMX OR AD NUMBER)	(CATEGORY)

RE-ORDER NO. 61-563

LUNAR PHYSICAL PARAMETERS STUDY

PARTIAL REPORT NO. 13

BREADBOARD DEVELOPMENT AND TESTS OF SUBSURFACE THERMAL APPARATUS

WORK PERFORMED UNDER J.P.L. CONTRACT NO. N-33552

SEPTEMBER 20,1961

TEXACO
INC.

RESEARCH AND TECHNICAL DEPARTMENT

EXPLORATION AND PRODUCTION RESEARCH DIVISION

BELLAIRE, TEXAS

This work was performed for the Jet Propulsion Laboratory, California Institute of Technology, sponsored by the National Aeronautics and Space Administration under Contract NAS7-100.

1443

RE-ORDER No. 61-563

LUNAR PHYSICAL PARAMETERS STUDY

PARTIAL REPORT NO. 13

BREADBOARD DEVELOPMENT AND TESTS OF SUBSURFACE THERMAL APPARATUS

WORK PERFORMED UNDER J.P.L. CONTRACT NO. N-33552

SEPTEMBER 20,1961

2

BREADBOARD DEVELOPMENT AND TESTS OF SUBSURFACE THERMAL APPARATUS

TABLE OF CONTENTS

BREADBOARD DEVELOPMENT AND TESTS OF SUBSURFACE THERMAL APPARATUS

Introduction

This report is an extension of Lunar Physical Parameters Study, Partial Report No. 8, Design Calculations, Measurement of Thermal Diffusivity. In describing apparatus for measurement of thermal diffusivity within a drilled hole, Partial Report No. 8 ended with a description of heat flow studies using copper shapes buried in unconsolidated materials.

To simulate borehole conditions, the proposed diffusivity units were suspended in glass tubing (1-1/8 in. I.D.) evacuated to a pressure in the range 10^{-5} - 10^{-6} mm of mercury, the glass tubing in turn being surrounded by materials of varying thermal conductivity. At constant energy input, the temperature rise of the copper shape system was insensitive to the conductivity of the medium surrounding the glass tubing. Heat transfer from the unit to the wall of the simulated borehole is by radiation, and in the case of reasonable power dissipations within the copper mass (on the order of 0.5 watt) long time periods are required to attain temperatures of the mass at which a significant net heat transfer by thermal radiation to the wall takes place. In periods of an hour no significant differences in temperature attained were noted within the proposed unit although the conductivity of the medium surrounding the glass tubing was changed from $2.9 \times 10^{-4} \frac{\text{cals}}{\text{cm sec.}\,^\circ\text{C}}$ to $8.8 \times 10^{-4} \frac{\text{cals}}{\text{cm sec.}\,^\circ\text{C}}$.

It was necessary to find a source of low mass capable of attaining high operating temperatures with low energy consumption, the high operating temperatures assuring efficient radiant energy transfer to the borehole wall. Various tungsten filament systems were operated and measurements of temperature rise at the borehole wall indicated a significant variation, at constant energy to the source, with the conductivity of the surrounding medium. Since in proposed operation within a hole drilled into the lunar material no contacting device can be used to estimate wall temperature, it is necessary that the unit itself respond to variations in the thermal conductivity of the surrounding medium. The temperature rise of a point on the unit was sufficiently sensitive to respond to a change in thermal conductivity from 2.9×10^{-4} cals/cm sec.°C to 8.8×10^{-4} cals/cm sec.°C, but did not respond to a change from 2.9×10^{-4} cals/cm sec.°C to 1.4×10^{-4} cals/cm sec.°C. However, temperatures taken at the glass wall gave evidence of significant changes in this last mentioned low range of thermal conductivity. Thus, a suitable source of energy was at hand, giving significant wall temperature variations between conductivities of 1.4, 2.9, and 8.8×10^{-4} cals/cm sec.°C, but it was necessary to build into the conductivity device a means of accurately sensing wall temperature variations. A radiometer was developed which gave a response proportional to the temperature difference existing between conductivity device and bore wall. This radiometer is a simple four junction thermopile system (iron-constantan) having a blackened copper square target about 1/4 in. on the side. No focusing optics were used. Since measurements of conductivity were taken for long time periods at the powers used, it was the original thought that a massive, slow response time radiometer would be adequate to the task. In the course of this work it was discovered that wall reflectivity influenced the measurement of thermal conductivity by affecting the energy absorbed, and that the reflectivity could be estimated from the initial step response of the radiometer, but to adequately correct out this variable would require considerably shorter time constant radiometers. This is then a necessary development before final flight units are built.

The devices for thermal measurements downhole were proposed for estimating thermal diffusivities of the lunar materials. However, the considerable mass of the measuring unit influences the temperature rise on the wall to the extent that the measurement is, at present, useful only as an empirically calibrated device responding to the conductivity of the surrounding materials.

A unit was assembled which demonstrates feasibility and ultimate practicability of the measurement of thermal conductivity from the downhole sonde. The radiometer included within this device serves to measure bore wall temperature. With the unit developed, an estimate was made of effects of positioning in borehole, borehole size, and effects of bore wall reflectivity.

Considerable amplification of the work performed to date is needed in:

1. Development of a radiometer unit having fast time constant.
2. Investigation of heat source configurations and geometry (possibly leading to elimination of bore-hole size as a parameter by directing radiation to a narrow sector).
3. Preparation of suitable calibration samples and independent determination of their thermal properties.
4. Set up of satisfactory calibrating and testing procedures for the ranges of environmental variables expected.

Sonde Unit Description

In developing the conductivity unit for placement in the sonde several sets of experiments were run for magnitude estimates of effects. In several cases time did not permit extension of an investigation to a logical end, but sets of partial investigations will be reported where it is felt that results obtained would be of interest in further development or would be helpful in interpreting behavior of the instrument completed for breadboard.

The sketch of Fig. 1 illustrates the simple set up used in the experiments involving downhole thermal properties.

The container was packed loosely with materials of the following description and properties:

TABLE I

Description of Material	Density gms/cm^3	Thermal Conductivity cals/sec cm°C
Clemtex No. 3 Blasting Sand	1.54	8.8×10^{-4}
Sil-O-Cel C-3	.49	2.9×10^{-4}
Styrofoam (unconsolidated)	.030	1.4×10^{-4}

The vacuum system involves a Welsh Duo-Seal fore pump, and a two-stage mercury diffusion pump with appropriate liquid nitrogen traps with which it was possible to work in the pressure range of 10^{-5} - 10^{-6} millimeters of mercury.

The conductivity device placed in such a system is not viewing directly a variation of bore wall properties, but, since in each case the glass tubing simulating borehole is present, is viewing a variation in properties of the surrounding medium through glass of several millimeters thickness. This system would not be useful for a direct empirical calibration, but it does allow evaluation since the presence of the glass tubing minimizes rather than accentuates the effect of changing medium properties.

There is the great advantage of ability to change the unconsolidated surrounding medium rapidly without breaking vacuum in the borehole simulation system.

Fig. 2 is a drawing of the first model of a downhole conductivity device. The radiometer assembly is a four-junction iron-constantan thermopile, the sensor target being a square of copper sheet approximately 1/4 in. on a side. The target on this first unit was coated with a white paint, thus being non-absorbing in the visible, but absorbing in the infrared. Fig. 3 shows the second model of conductivity device as assembled into the sonde. It differs from the first model in sensor coating, this unit being painted with "Aqua-Dag", an aqueous suspension of colloidal graphite in water, and also it differs in dimension, being reduced to the 7/8 in. diameter of the sonde. Provision was made in this sonde device for inclusion of an infrared transparent shield to be of KRS-5 or similar material necessarily furnished by sub-contractor. Fig. 4 illustrates the circuitry associated with use of this downhole device. The thermopile in the sonde unit is a four-junction chromel-constantan system.

Use of the Downhole Conductivity Unit

The General Electric automotive bulb (#57) used in this apparatus had the following characteristics at the given outputs:

TABLE II

Current (Amperes)	Voltage (Volts)	Resistance (Ohms)	Power (Watts)
0.120	4.2	35	0.50
0.156	6.5	42	1.01
0.187	8.6	46	1.61

The variation in resistance with power level results from the change in operating temperature of the tungsten filament. A change in the effective blackbody emission of the filament is associated with a change in power level, and it should be kept in mind that absorption characteristics of surfaces have wavelength dependence, which means that power level changes at the filament affect energy absorbed by the surrounding wall by varying not only the energy available, but also its wavelength distribution.

Operation of the various forms of conductivity devices within the vacuum system was quite simple. The unit was suspended by its connecting wires at the desired height in the tubing. Wires leading out of the vacuum system were provided for the power to the device, thermocouple reading at the device, and thermopile reading from the unit. A thermocouple for reading what has been termed, "wall temperature", was fastened on the outer surface of the glass tubing simulating borehole. This is the temperature at the interface between the glass tubing and packed unconsolidated medium. Fig. 4 illustrates the circuitry used and requires little explanation. The divider circuit labeled, "reference voltage", was useful in extending the range of the dual channel recorder by cancelling out known quantities of thermocouple outputs. Further description of operation will be given under other headings.

Effect of Positioning in Simulated Borehole

During early work using a 110 volt pilot lamp at power levels of about 1.6 volts, it was found that shielding above the bulb and operation at hole bottom gave significantly less temperature variation at the wall with conductivity of the surrounding medium than operation at levels above hole bottom with confining shields above and below the heat source. This led to a decision to place the thermal device above the radiometer in the sonde sequence, with shielding to confine heating to a cylindrical region around the bulb. Development of the device continued with this positioning in mind.

Effect of Bore Diameter

Figs. 5 through 8 illustrate effects of bore size variation and also effects of reflectivity. Curves taken from the thermal devices are of this type, and will have illustrated the wall temperature, taken at the glass wall-unconsolidated medium interface at the location of the thermal device, and the assembly temperature, a thermocouple reading at the reference junctions of the thermopile within the thermal unit. The radiometer output is the thermopile signal, which is a function of the temperature difference between the target and the assembly, this difference being generated by the radiation interchange between target and wall. Note that these curves include data taken directly on the bore wall, but in the anticipated use this information will be lacking. The device is practical only if it is possible to predict accurately wall temperature from the other two curves, assembly temperature and radiometer output. The thermal device was fitted with a decentralizing spring so that even with change in bore diameter the radiometer side of the device was pressed against the bore wall. The unit used in this set of experiments had a sensing target with white coating, this minimizing the contribution of reflecting light. Comparing Figs. 5 and 6, and Figs. 7 and 8, illustrates the variations in temperatures expected from this geometry with a change in bore inner diameter from 1-1/8 in. to 1-9/16 in., holding other variables constant. Figs. 5 and 7, and Figs. 6 and 8, exhibit the variations in temperatures seen as a result of changing the absorption characteristics of the surrounding medium, this being accomplished by coating the exterior surfaces of the glass tubing with "Krylon" flat black paint.

The radiometer output and assembly temperature (from which must be deduced the wall temperature, the desired information) are sensitive with a given power input to the bore diameter and the absorption characteristics of the surrounding wall for the emitted spectrum of the filament. A possibility exists of making the device relatively insensitive to bore diameter by focusing the emitted radiation on a portion of the wall, the area irradiated being changed only slightly by variation in bore diameter. If this is impractical, it will be necessary in the empirical calibration to account for bore diameter and absorption characteristics. This is possible since bore diameter is part of the data obtained by the sonde, and a means of estimating wall reflectivity will be discussed in a later section.

Conductivity Determinations

Figs. 9 through 19 illustrate the practicality of determining thermal conductivity by use of a device of the form of Fig. 2 (assembly with white target). The device was operated at power levels of roughly 0.5, 1.0, and 1.6 watts (14.3 cals/min = 1 watt) in a bore approximately 1-1/8 in. inner diameter, with surrounding materials of 1.4, 2.9, and 8.8 x 10^{-4} cals/cm sec.°C. In this series, Figs. 11 and 12, 14 and 15 are attempts at duplication, allowing estimate of reproducibility. In these curve sets the radiometer signal appears proportional to the difference in wall and assembly temperatures, such that prediction of wall temperature from assembly and radiometer signals seems feasible. No attempt was made to accurately calibrate this device, but immediately the device of Fig. 3 was built, having a blackened (Aqua-Dag) sensor element.

Operation of the device of Fig. 3 resulted in the curves of Figs. 20 through 27, Figs. 20 through 23 involving use of the isolated device, Figs. 24 through 27 involving use of the device assembled within the sonde.

Considering Figs. 20 through 23, the low mass of the sonde allowed the assembly temperature to rise above the wall temperature. Abrupt signal reversals were experienced at the times the light bulb went on and off. These reversals were attributed to the reflected light from the wall contributing to the radiometer output, thus augmenting the thermal radiation from the wall. The radiometer in this case is a four-junction chromel-construction unit, with comparatively massive target. In radiometer work for these units no attempt had been made to form a sensitive, fast response unit requiring accurately formed optics. To obtain sensitivity, a massive, large area target was used. From Figs. 20 to 23, a time of about four minutes was deduced for this unit to respond to what must be almost a step function of reflective input.

When this unit was assembled into the sonde the heat taken up by the thermal device was conducted up into the sonde keeping assembly temperatures low. The reflective inputs in this

RE-ORDER No 61-563

case did not give reversals of radiometer output. This makes it difficult to analyze data as given in Figs. 24 and 25 where styrofoam and sil-O-cel seem to be giving almost identical radiometer and assembly outputs, although conductivity varies by a factor of about 2. That this is the result of absorption characteristics is shown by Figs. 26 and 27 where styrofoam and sil-O-cel were given the same absorption characteristics by coating the containing glass tube with flat black "Krylon" paint, and a clear distinction can be seen. Greater absorption resulted in higher wall temperature in these cases.

The obvious means of applying "reflectivity" corrections are to make prior calibration for reflectivity and additionally to improve the response of the radiometer such that step functions as given by the reflective component can be identified. The necessity of making this correction for reflectivity is obvious from comparing Figs. 24 and 26, and Figs. 25 and 27, where changes in absorption characteristics give different wall temperatures for equal heat inputs and equivalent surrounding thermal conductivities.

Responses of wall temperature for given heat inputs in times less than 10 minutes are comparatively low, something not expected if the system approximated a point source in an infinite medium. Since this approximation does not seem to hold, the diffusivities at short time would be primarily determined for sonde materials, leaving this device useful only as an empirically calibrated unit for thermal conductivity of surrounding materials.

Since several obvious development steps are required between breadboard and prototype models of conductivity device, steps requiring time not available under this contract, no further work was undertaken with the breadboard units.

RE-ORDER No 61-563

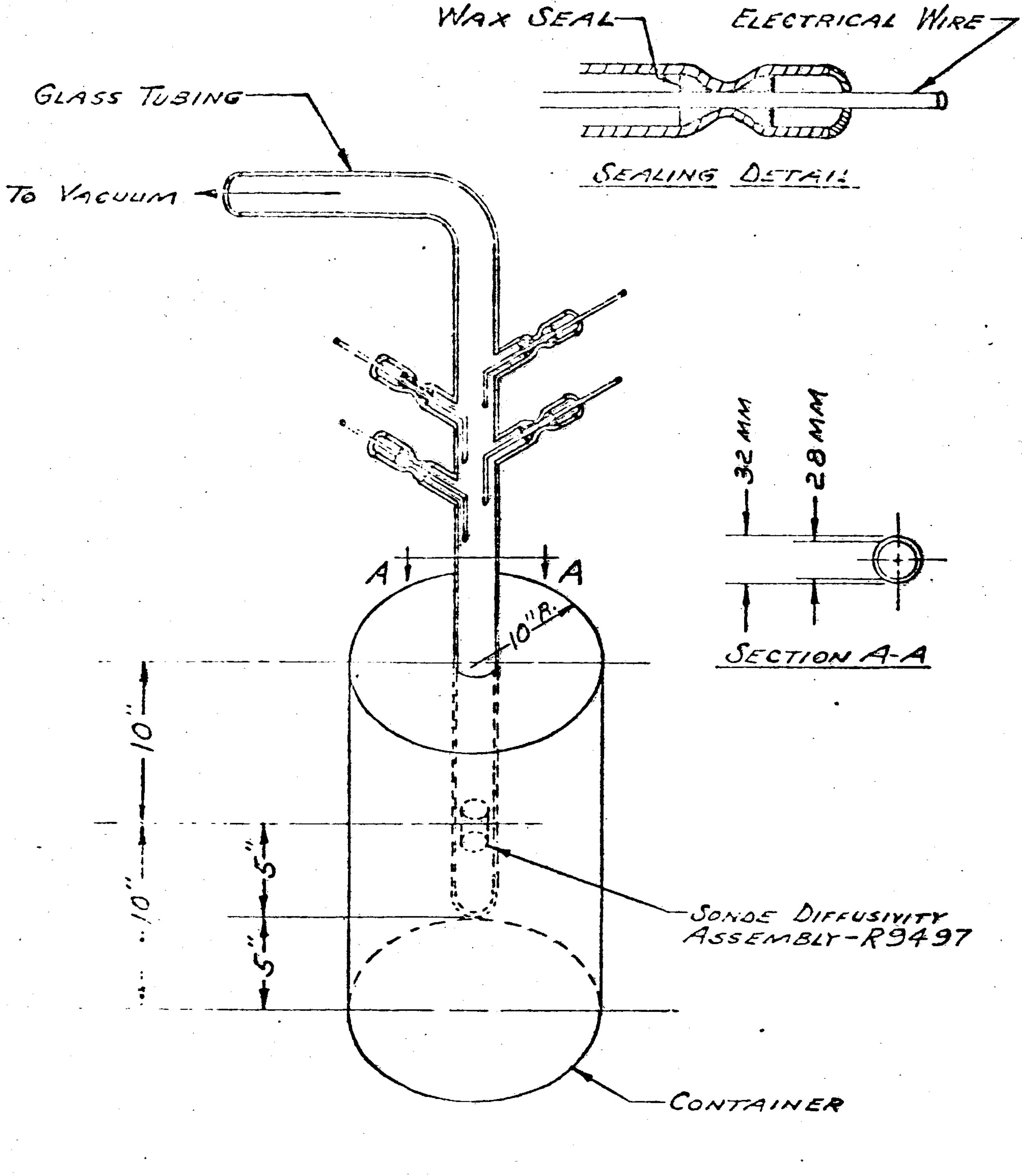

FIGURE 1

MATERIAL	SIZE	QUANT.	LET.	REVISIONS	DATE	BY

UNLESS OTHERWISE
ALL DIMENSIONS ARE
FRACTIONAL ±
DECIMAL ±
ANGULAR ±

SUPERSEDED BY
SUPERSEDES
CORRECT FOR N
FIRST INST. No

TEST CHAMBER
DOWN-HOLE DIFFUSIVITY ASS'Y.
T.B # N33552

TEXACO Inc.
RESEARCH AND TECHNICAL DEPARTMENT
EXPLORATION AND PRODUCTION RESEARCH DIVISION
BELLAIRE, TEXAS

DE. R.E.K. DR. B.D.S. TR.
CK. DATE: 27 JUNE '61
SCALE: NONE
ASSEMBLY NO. NONE

U9498 /17

RE-ORDER No. 61-563

81

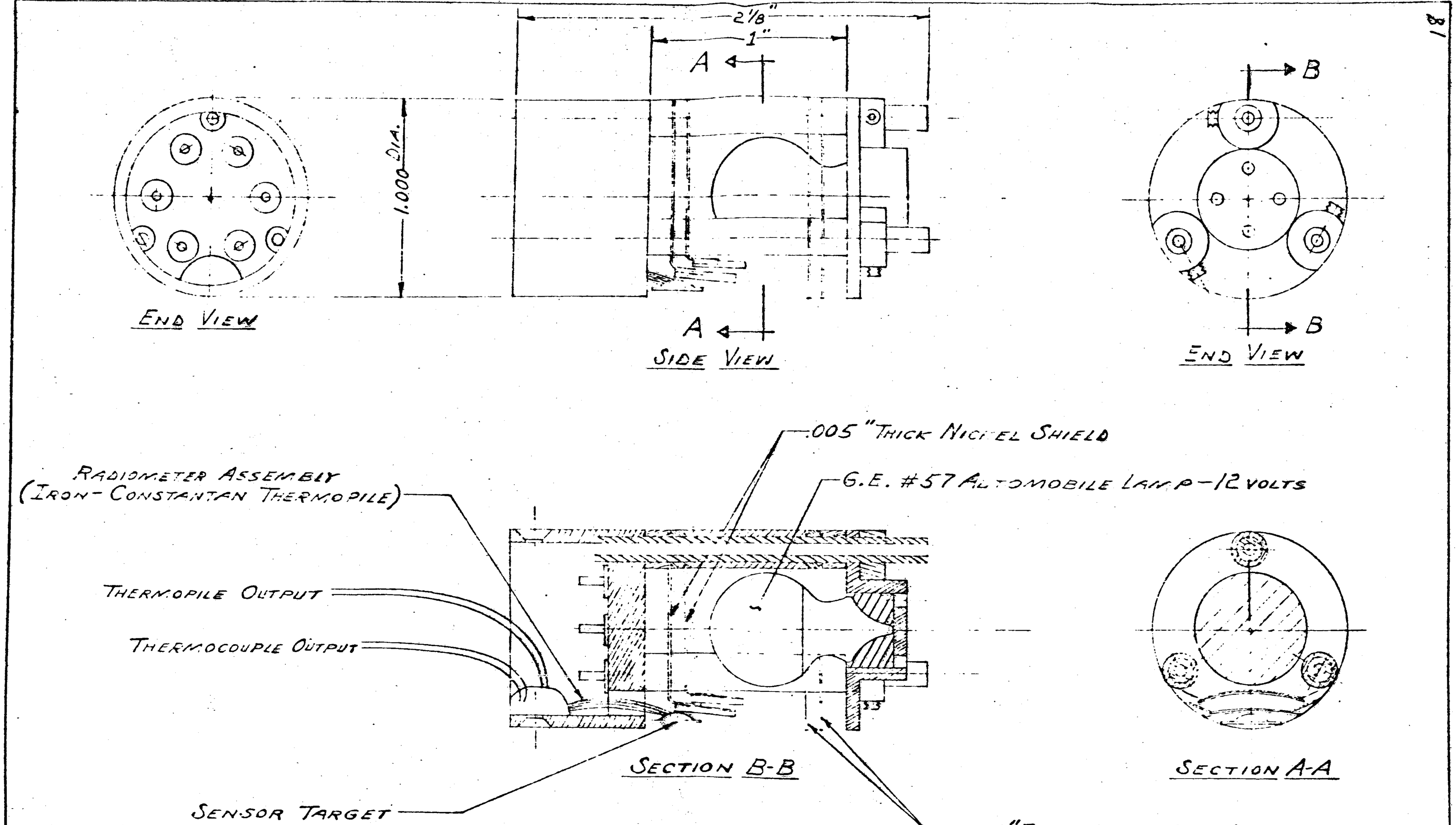

FIGURE 2

UNLESS OTHERWISE SPECIFIED ALL DIMENSIONS ARE:
FRACTIONAL ± 1/64" DECIMAL ± .005" ANGULAR ± 0° 30'

MATERIAL | SIZE | QUANT. | LET. | REVISIONS | DATE | BY

DESIGNED R.E.K. DATE 25 MAY '61 SCALE DOUBLE SIZE FIRST INST. NO. CORRECT FOR INST. NO. SUPERSEDED BY SUPERSEDES

DRAWN B.D.S. DATE 27 JUNE '61

TRACED DATE

CHECKED DATE

TEXACO
RESEARCH AND TECHNICAL DEPARTMENT
EXPLORATION AND PRODUCTION RESEARCH DIVISION
BELLAIRE, TEXAS

SONDE DIFFUSIVITY ASSEMBLY
MODEL I
JOB # N33552

ASSEMBLY RA9449

R9497

RE-ORDER No. 61-563

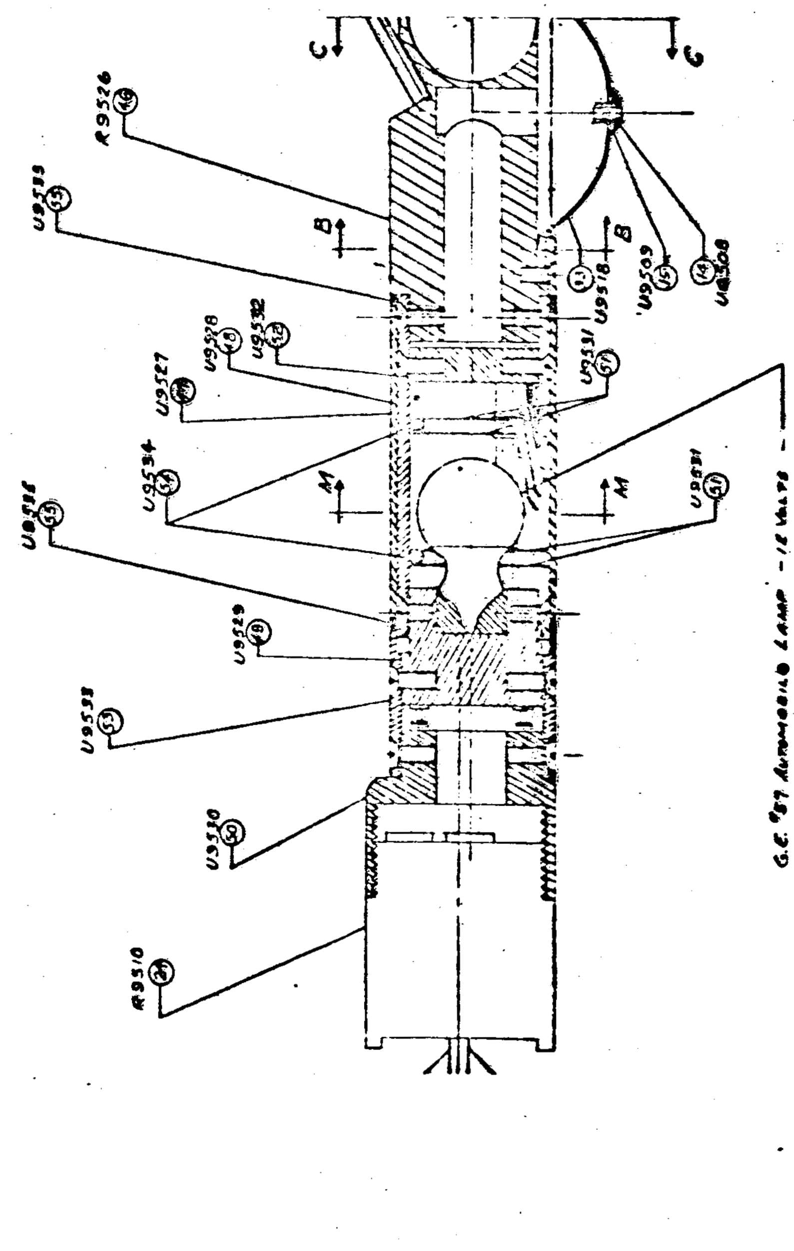

FIGURE 3

1:794-75
1:794.39-16

APPARATUS USED FOR DIFFUSIVITY MEASUREMENTS

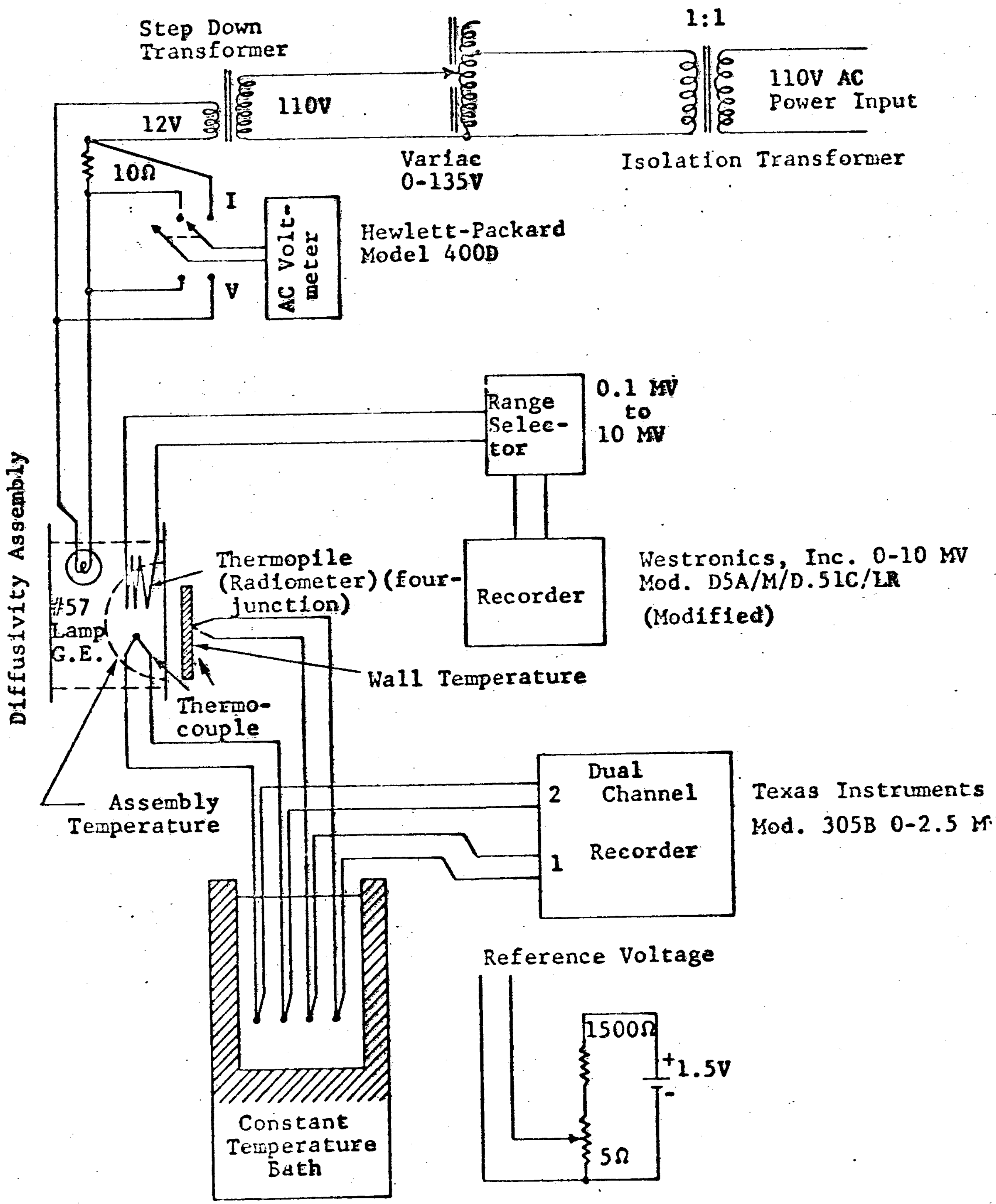

FIGURE 4

1:794.39-17
1.794-76

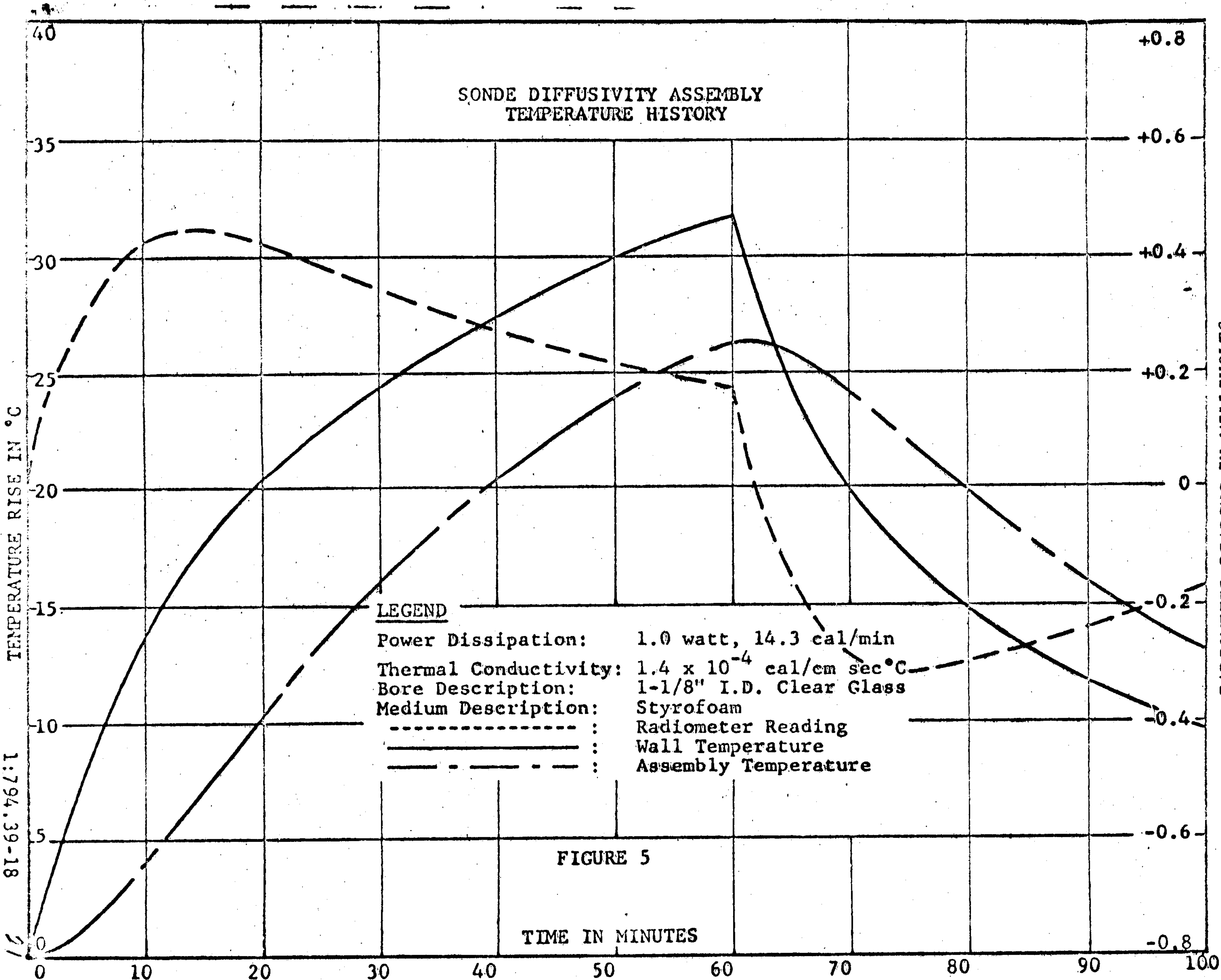

FIGURE 5

1:794.39-18

RE-ORDER No. 61-563

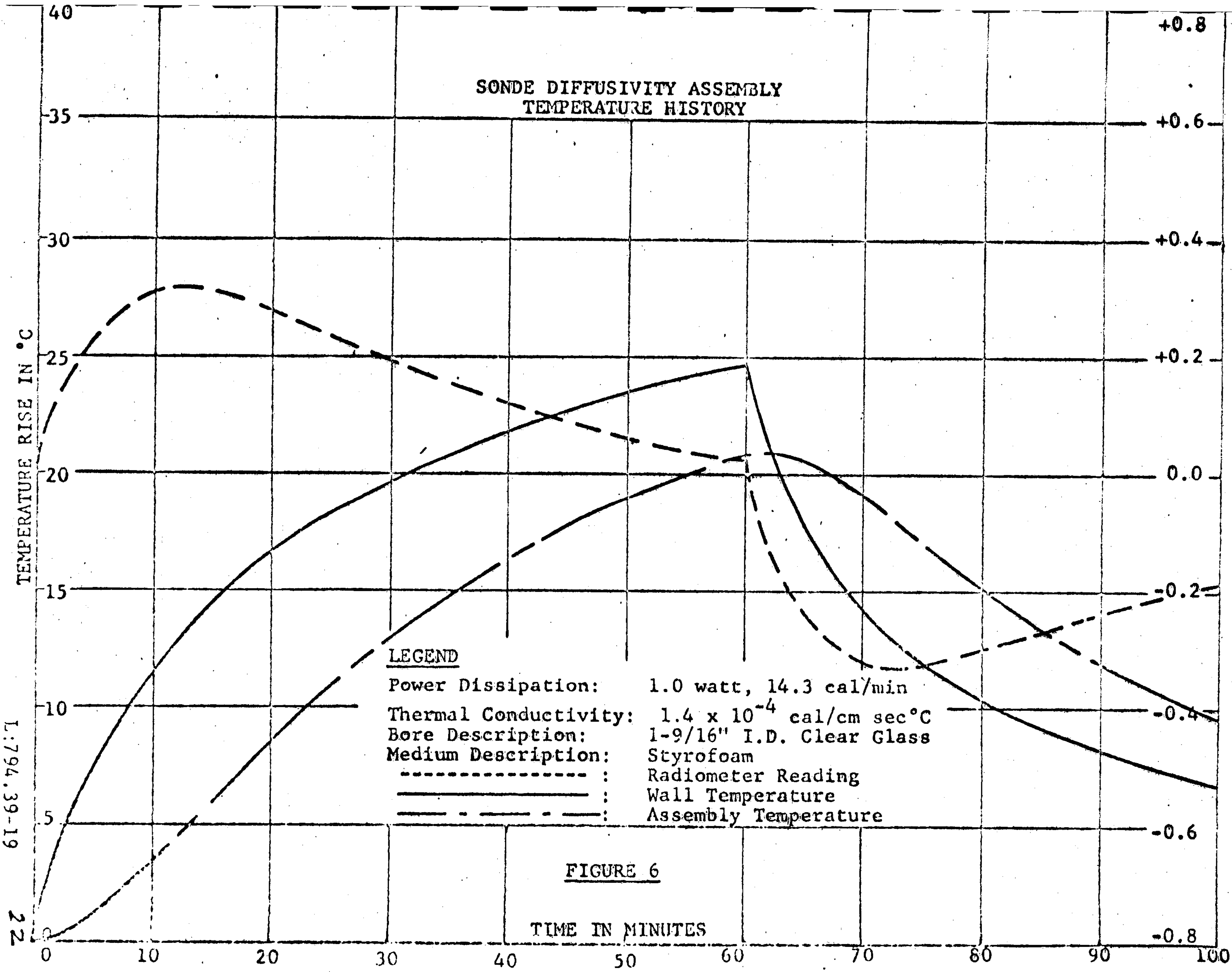
SONDE DIFFUSIVITY ASSEMBLY
TEMPERATURE HISTORY
TEMPERATURE RISE IN °C
40
35
30
25
20
15
10
5
0
RADIOMETER READING IN MILLIVOLTS
+0.8
+0.6
+0.4
+0.2
0.0
-0.2
-0.4
-0.6
-0.8
TIME IN MINUTES
10
20
30
40
50
60
70
80
90
100
LEGEND
Power Dissipation: 1.0 watt, 14.3 cal/min
Thermal Conductivity: 1.4 x 10^-4 cal/cm sec°C
Bore Description: 1-9/16" I.D. Clear Glass
Medium Description: Styrofoam
---------------- : Radiometer Reading
———————— : Wall Temperature
— — - — — - — : Assembly Temperature

FIGURE 6

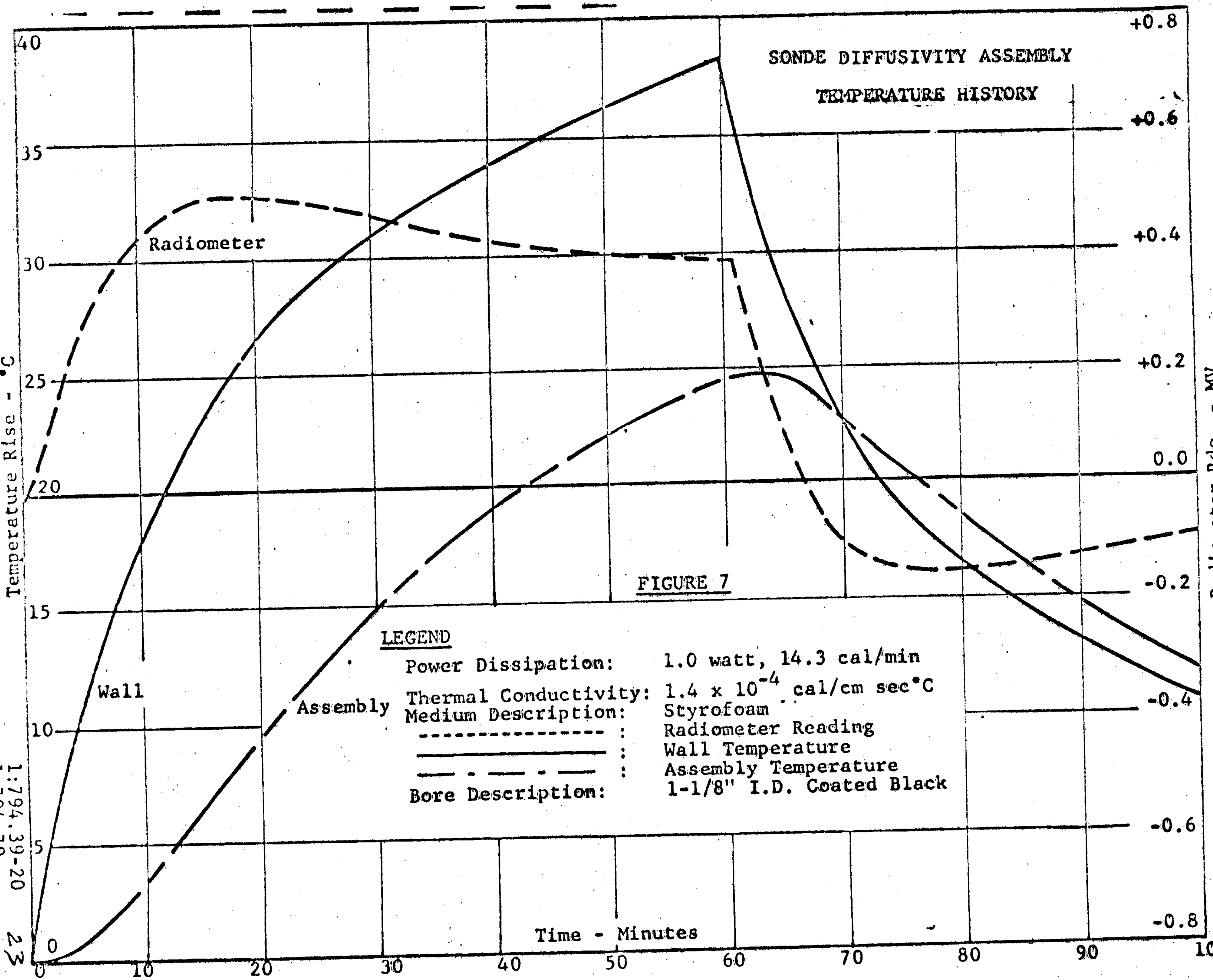

FIGURE 7

RE-ORDER No. 61-563

1:794.39-20
1.794-79

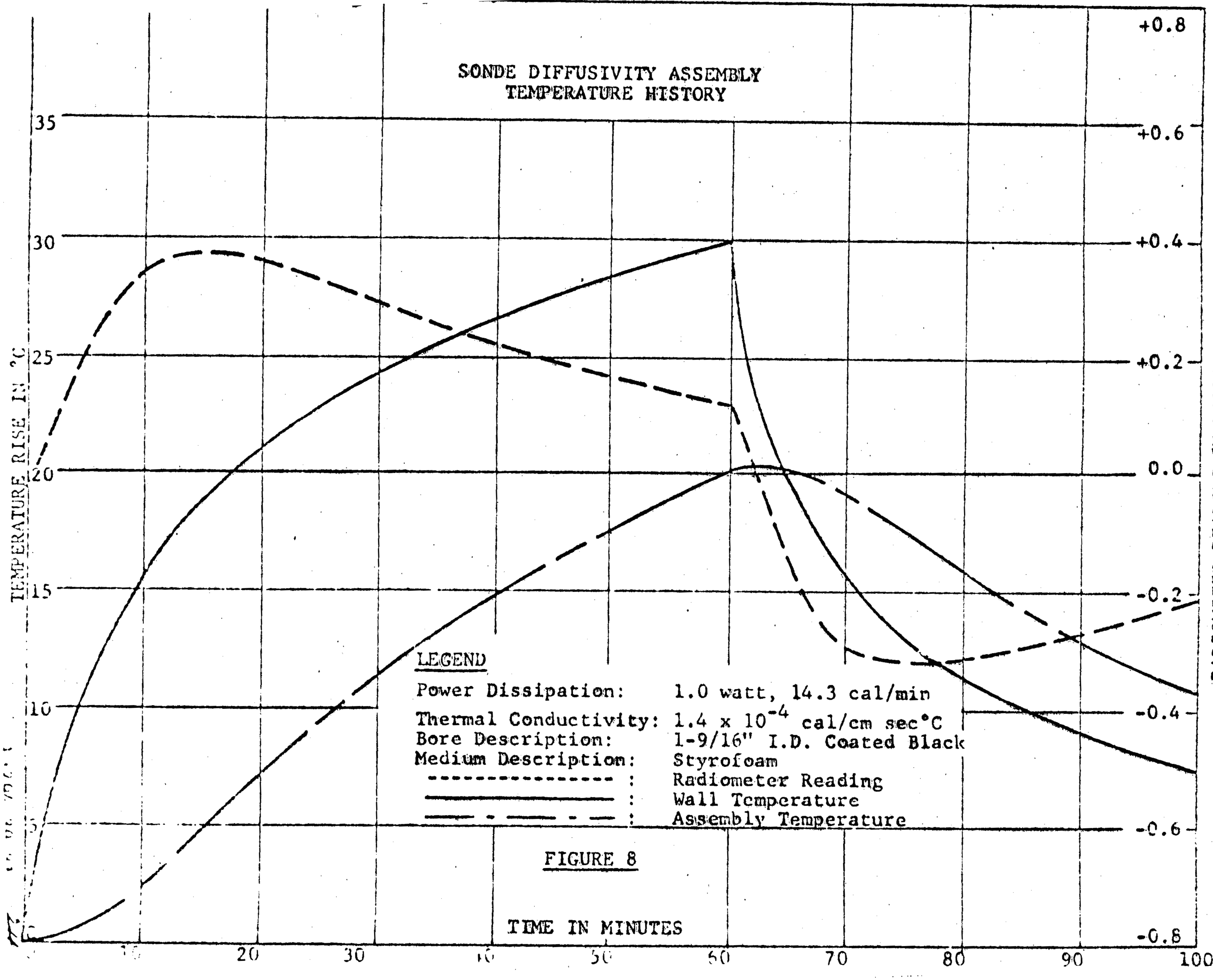

FIGURE 8

RE-ORDER No. 61-563

SONDE DIFFUSIVITY ASSEMBLY
TEMPERATURE HISTORY

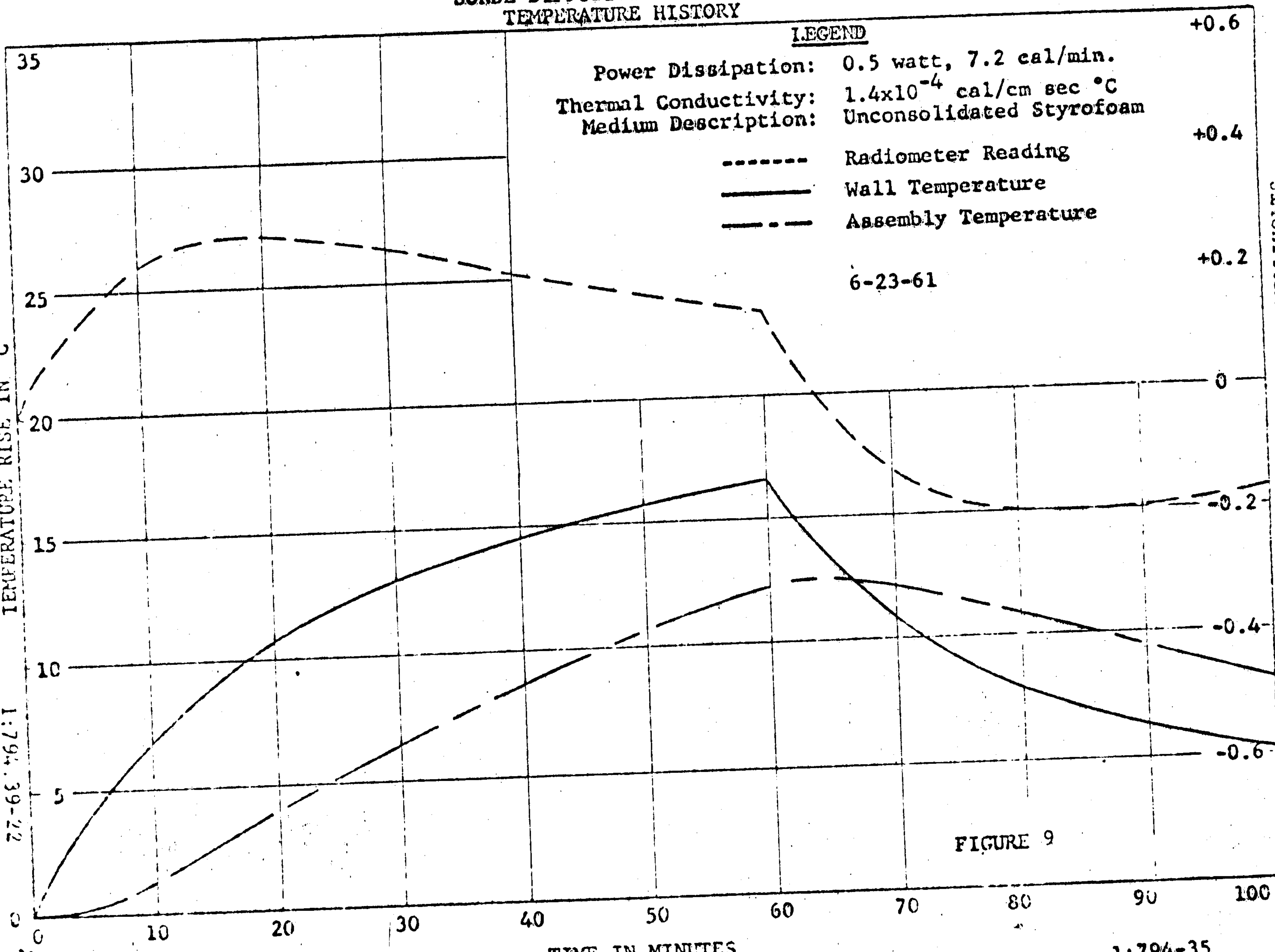

FIGURE 9

1:794.39-22
1:794-35

1:794-35

RE-ORDER No. 61-563

25

SONDE DIFFUSIVITY ASSEMBLY
TEMPERATURE HISTORY

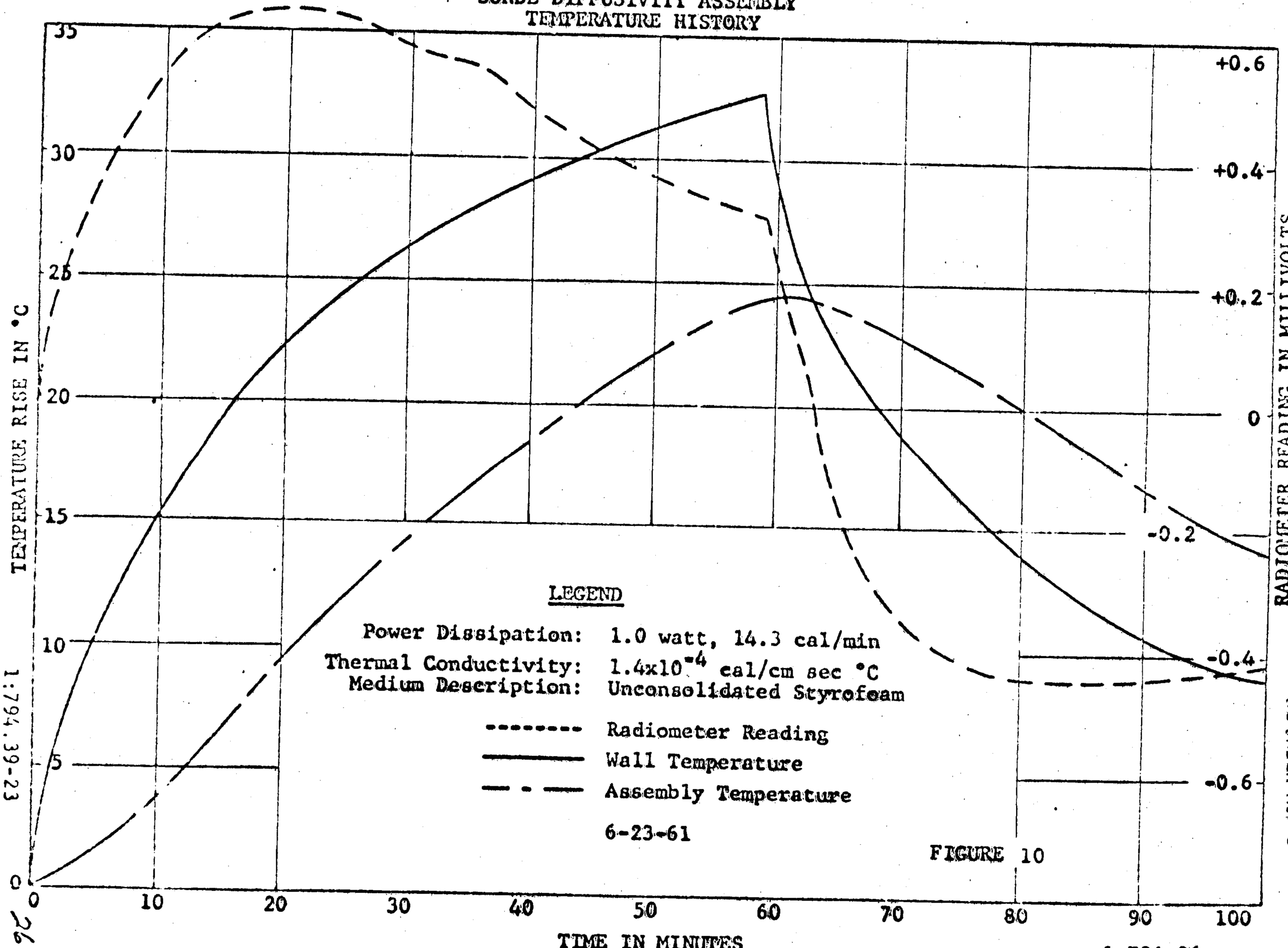

FIGURE 10

1:794-36

1:794.39-23
1:794-36

RE-ORDER No. 61-563

26

SONDE DIFFUSIVITY ASSEMBLY
TEMPERATURE HISTORY

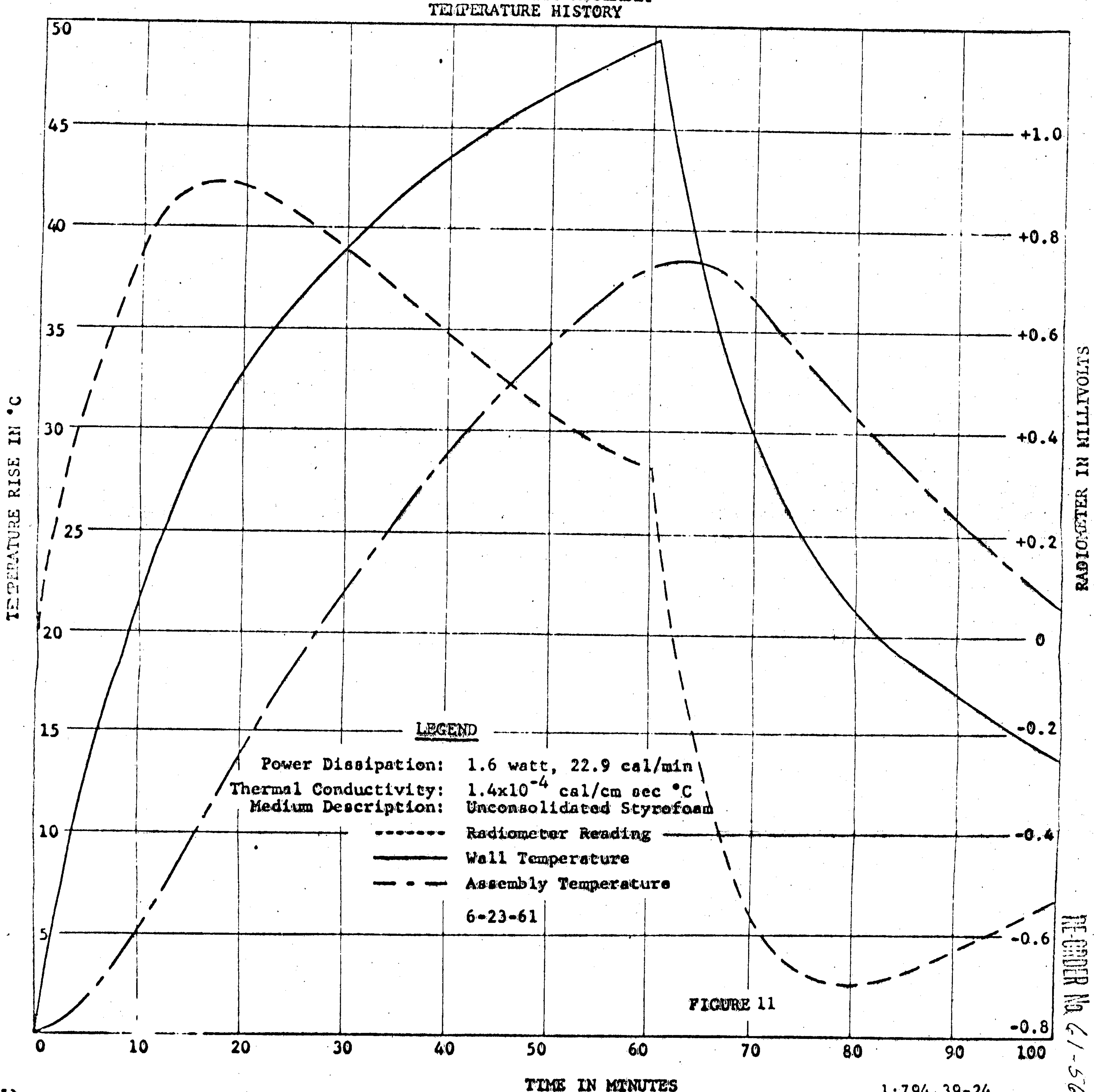

FIGURE 11

1:794.39-24
1:794-37

RE-ORDER No 61-563

SONDE DIFFUSIVITY ASSEMBLY
TEMPERATURE HISTORY

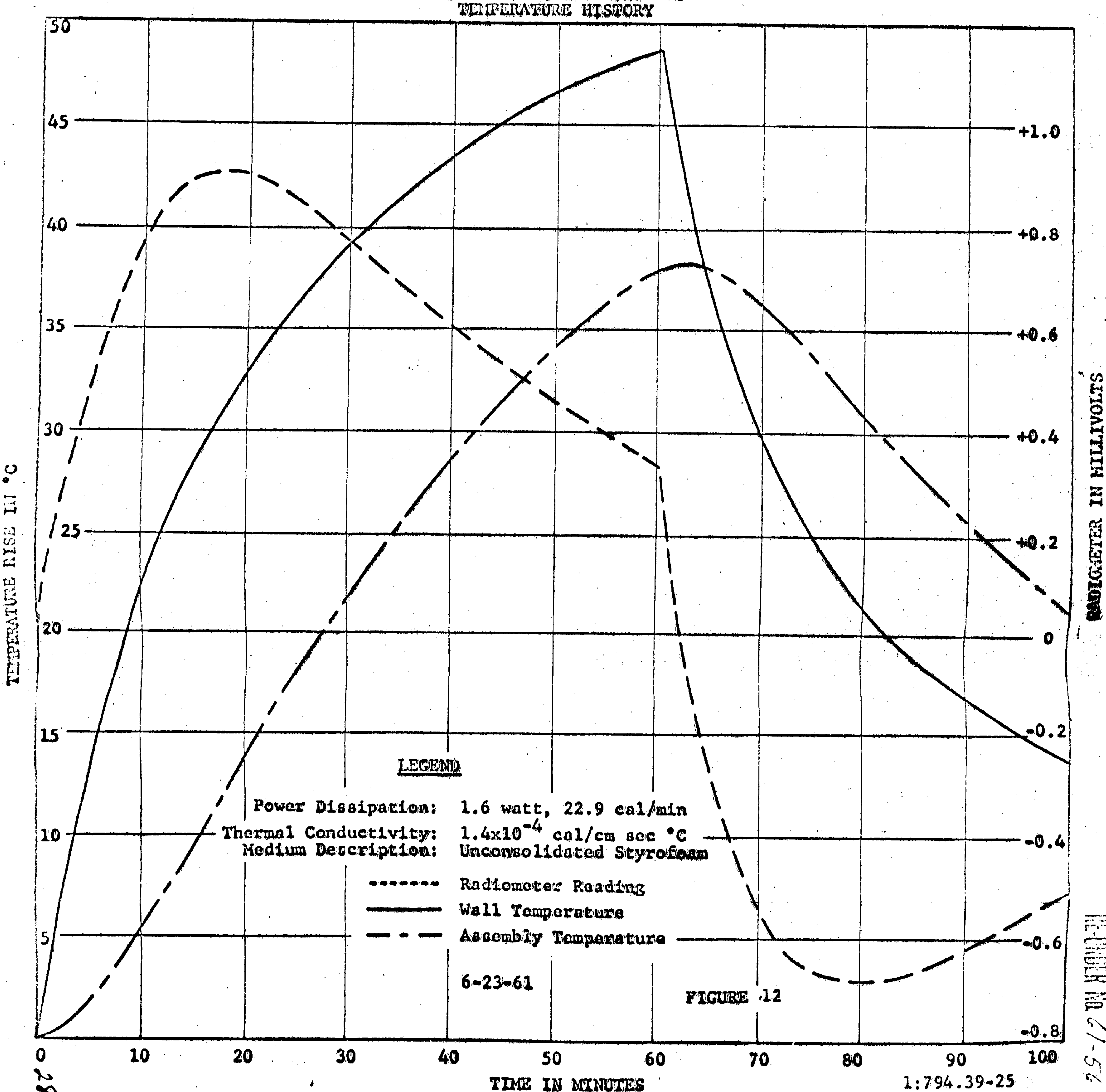

FIGURE 12

28

1:794.39-25
1:794-38

RE-ORDER NO. 61-56

SONDE DIFFUSIVITY ASSEMBLY
TEMPERATURE HISTORY

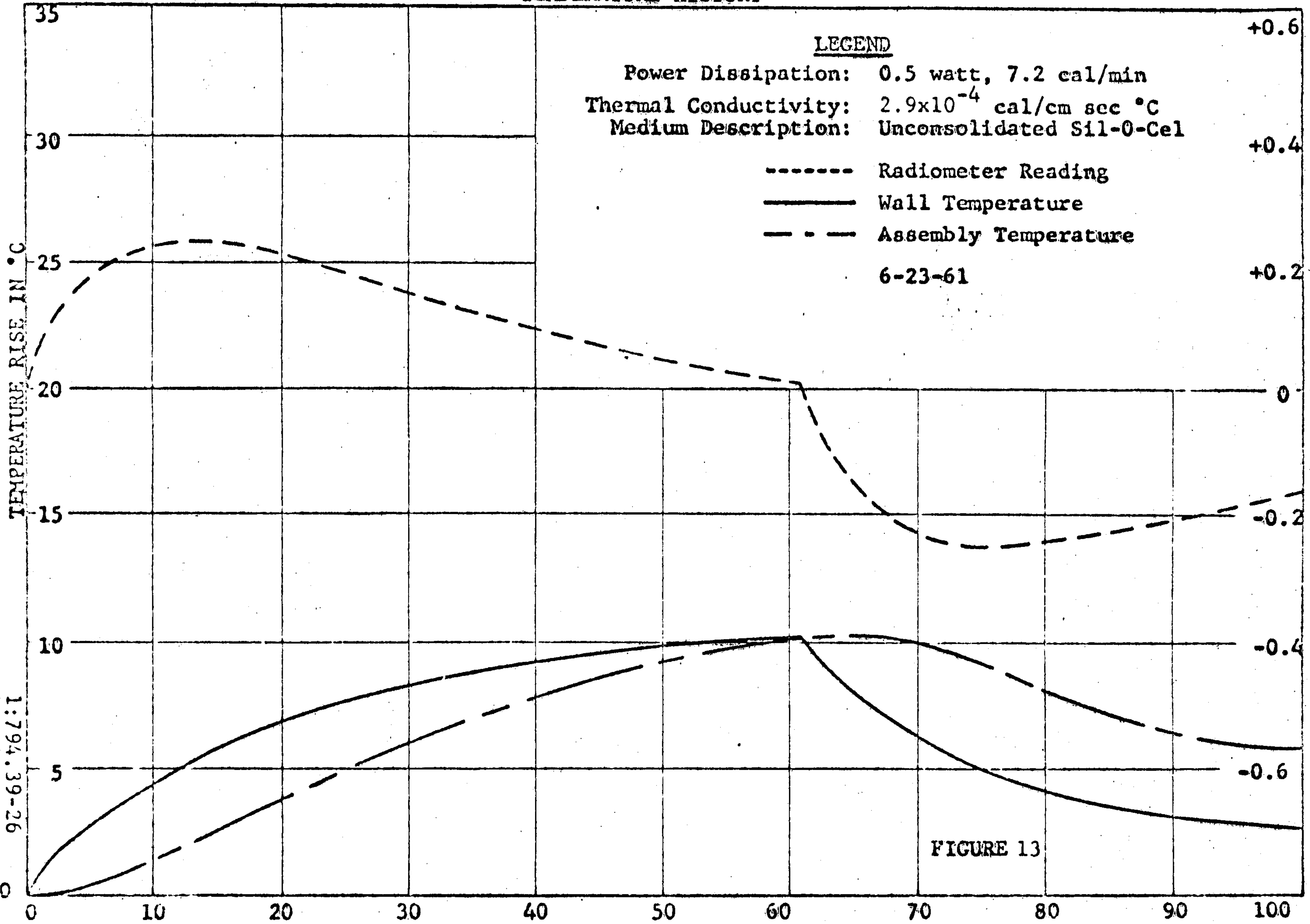

FIGURE 13

1:794-39

1:794.39-26
1:794-39

RE-ORDER No. 61-563

29

SONDE DIFFUSIVITY ASSEMBLY
TEMPERATURE HISTORY

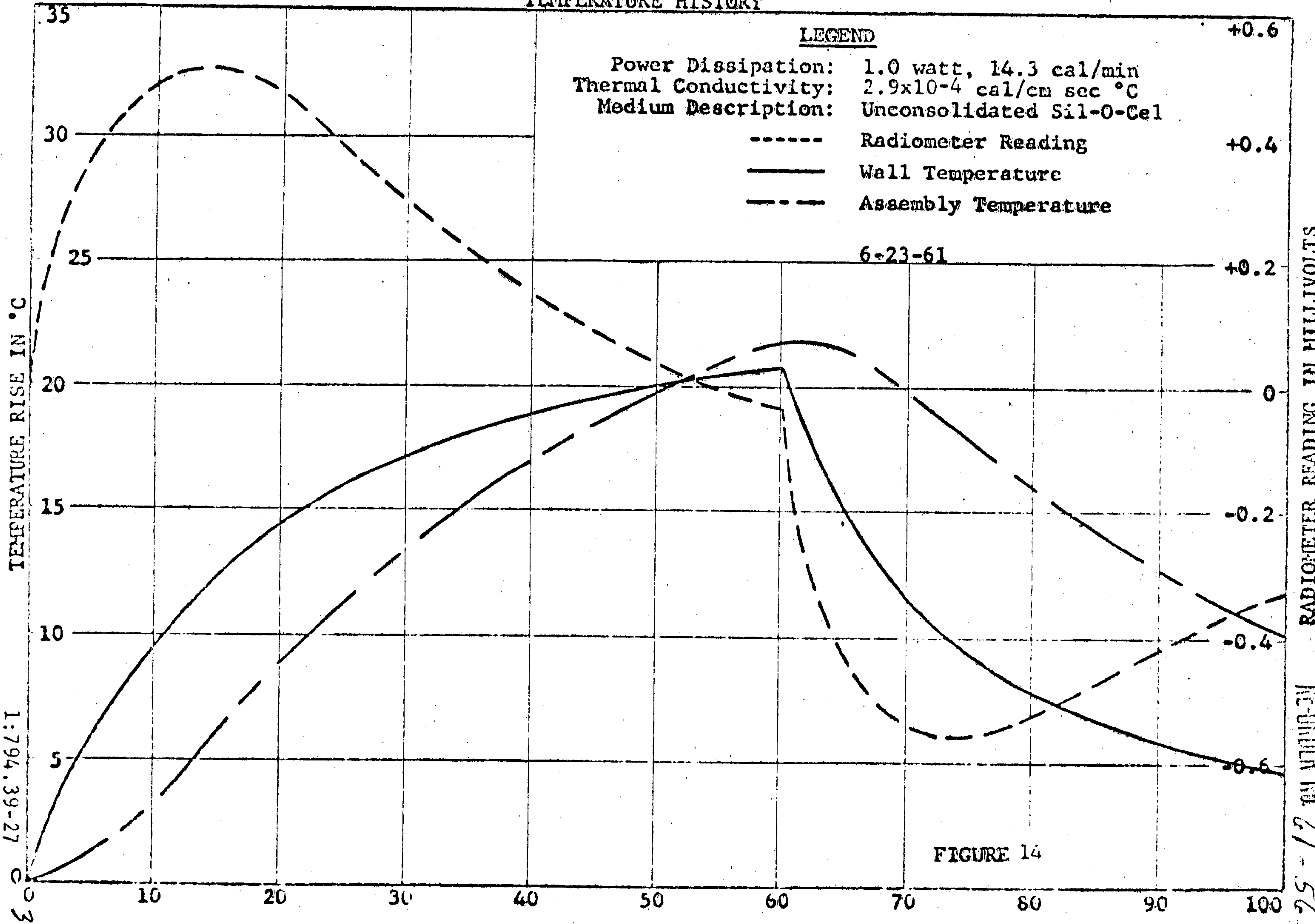

FIGURE 14

1:794.39-27
1:794-40

1:794-40

RE-ORDER No. 61-563

30

SONDE DIFFUSIVITY ASSEMBLY
TEMPERATURE HISTORY

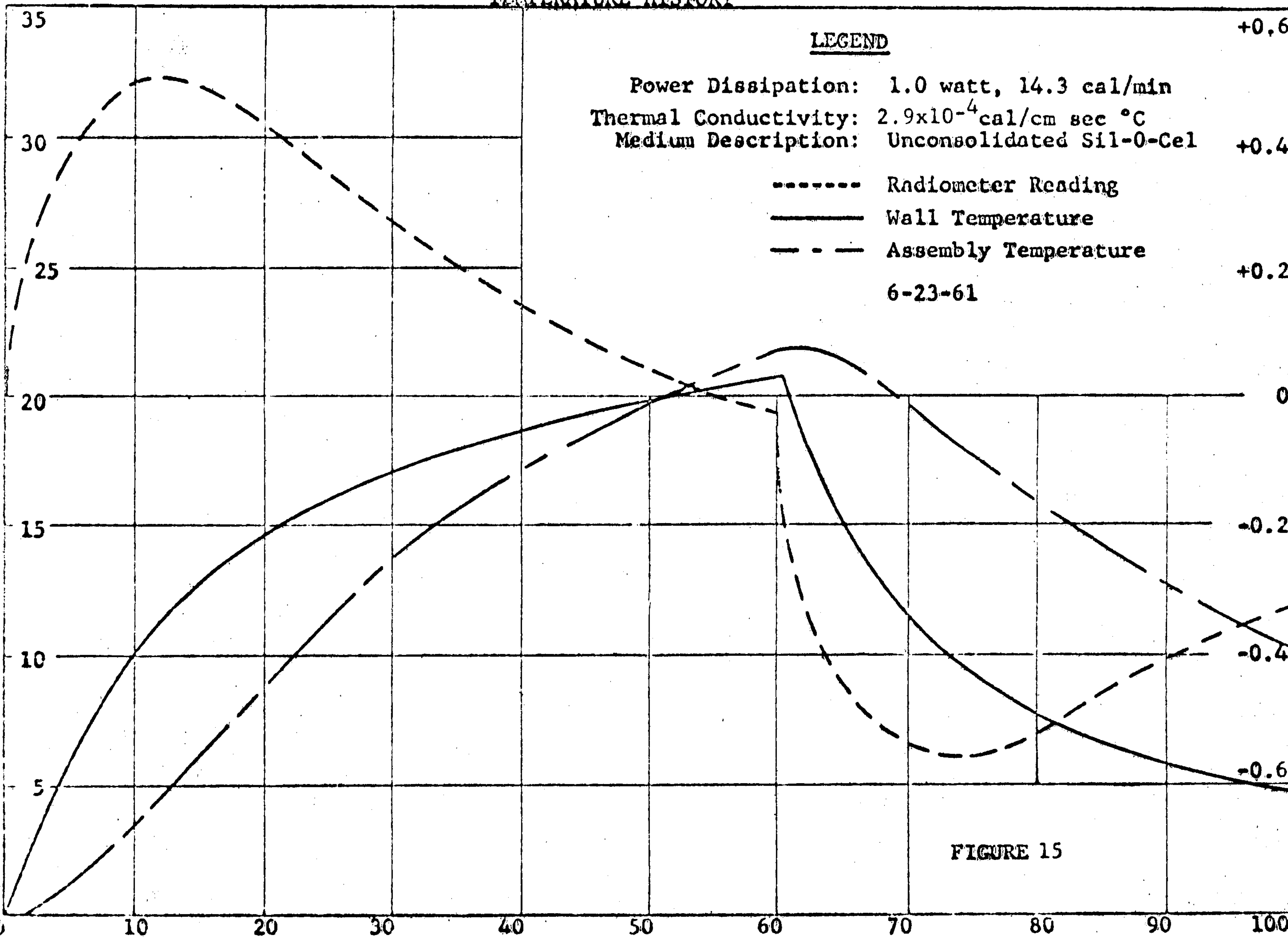

FIGURE 15

1:794.39-26
1:794-41

1:794-41

RE-ORDER No. 61-563

SONDE DIFFUSIVITY ASSEMBLY
TEMPERATURE HISTORY

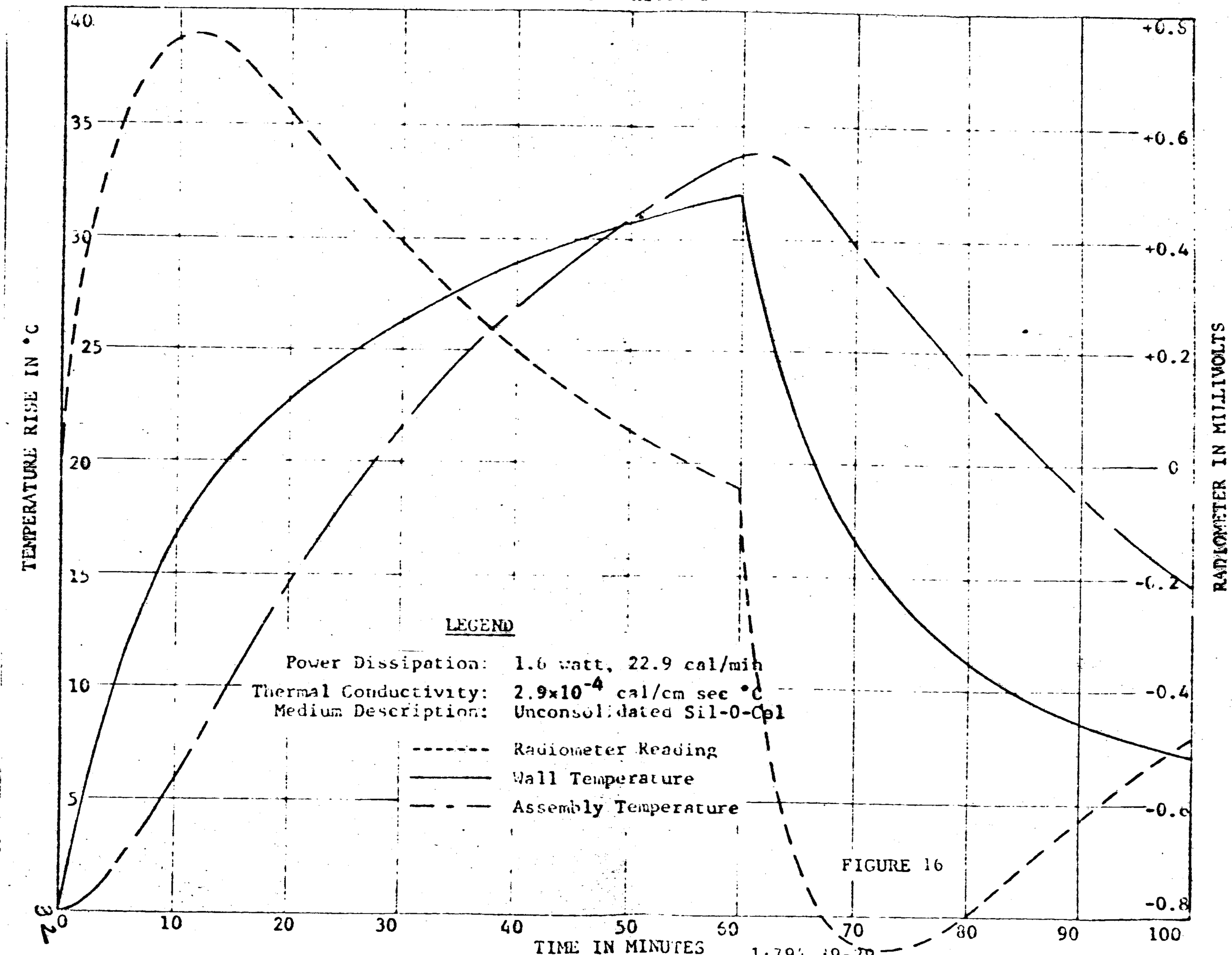

FIGURE 16

1:794.39-29

1:794-42

SONDE DIFFUSIVITY ASSEMBLY
TEMPERATURE HISTORY

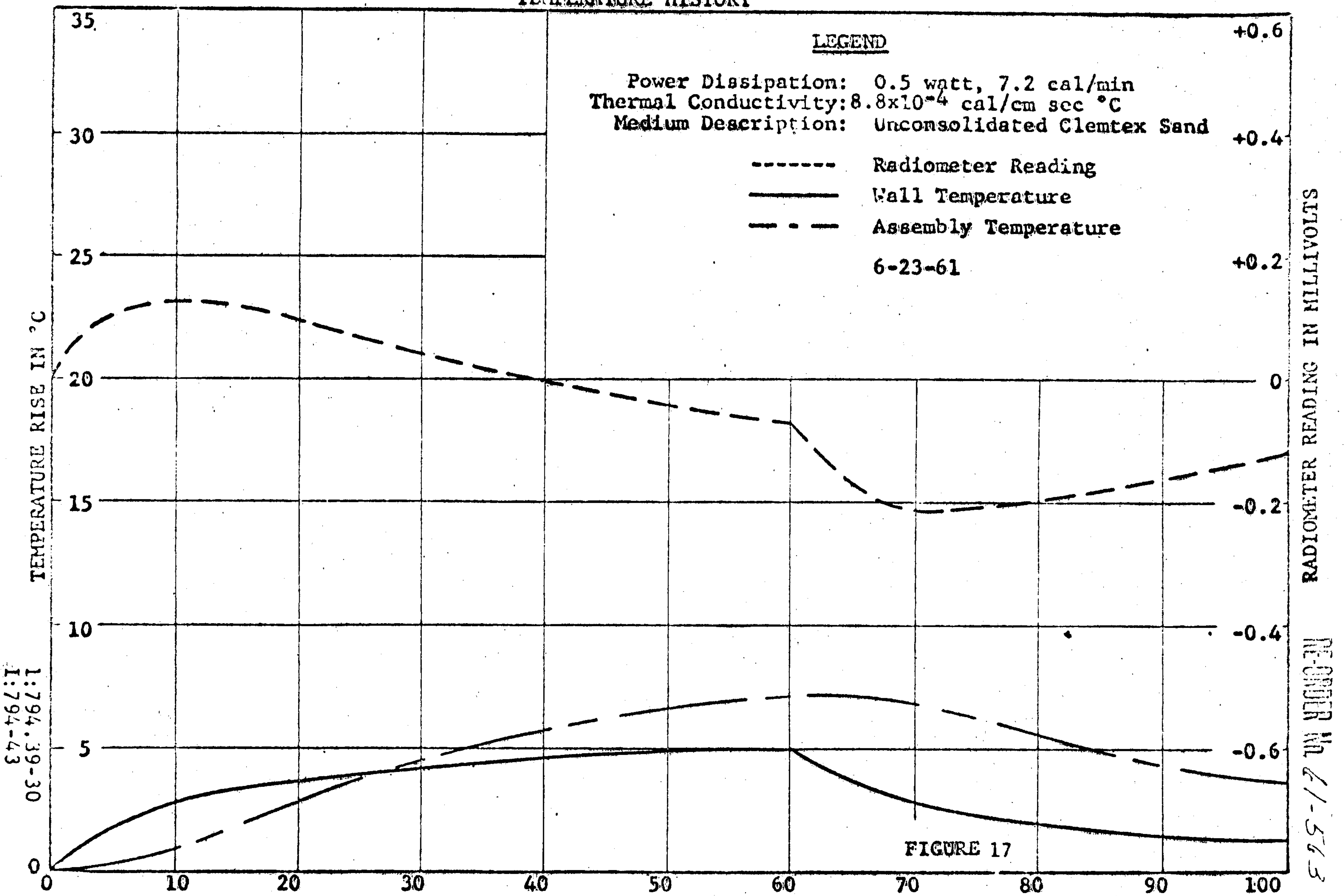

FIGURE 17

RE-ORDER No. 61-563

1:794.39-30
1:794-43

1:794-43

SONDE DIFFUSIVITY ASSEMBLY
TEMPERATURE HISTORY

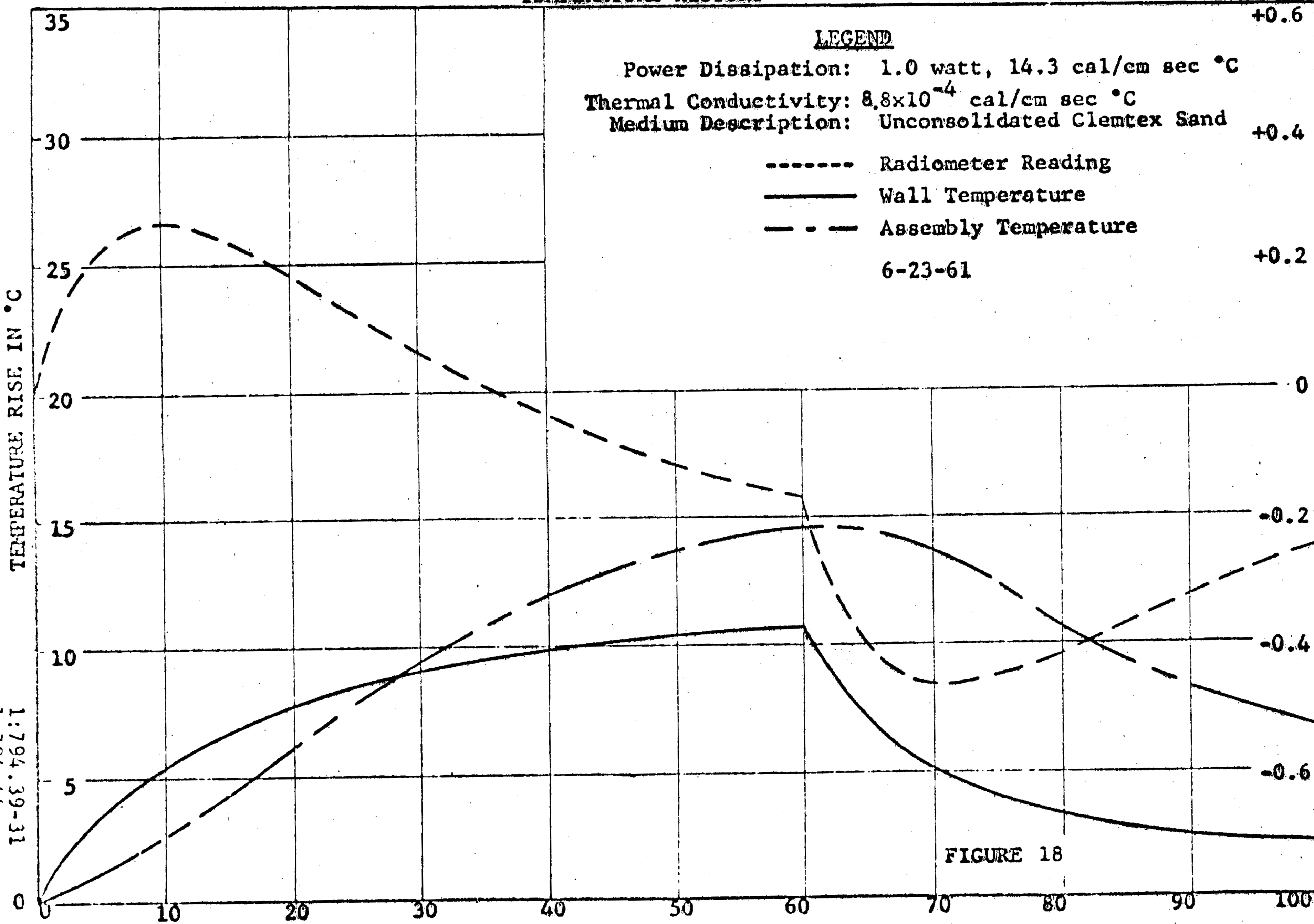

FIGURE 18

1:794-44

1:794.39-31
1:794-44

61-563

34

SONDE DIFFUSIVITY ASSEMBLY
TEMPERATURE HISTORY

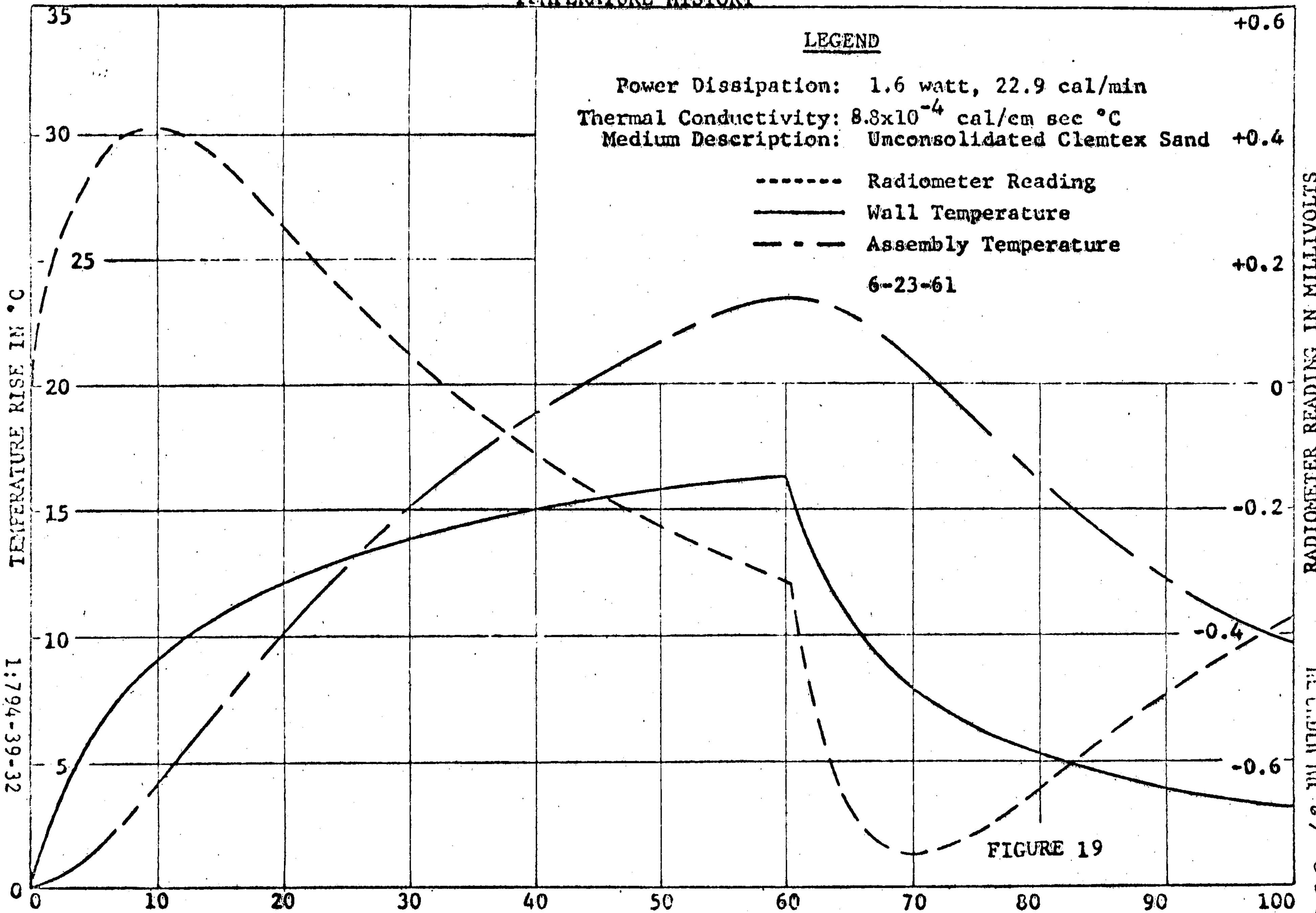

FIGURE 19

1:794-39-32
1:794-45

1:794-45

RE-ORDER No. 61-563

35

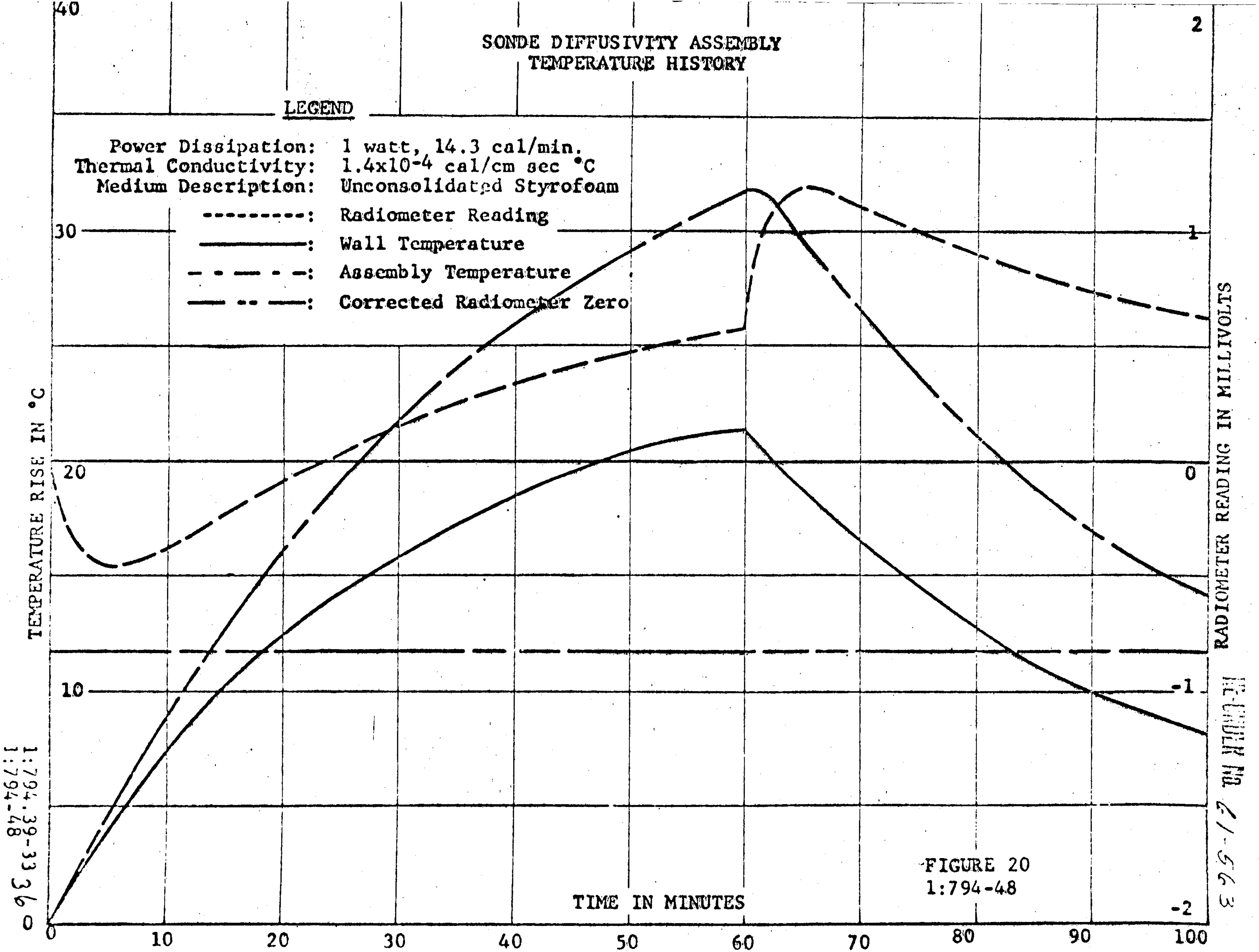

FIGURE 20
1:794-48

1:794.39-33
1:794-48
36

RE-ORDER No. 61-563

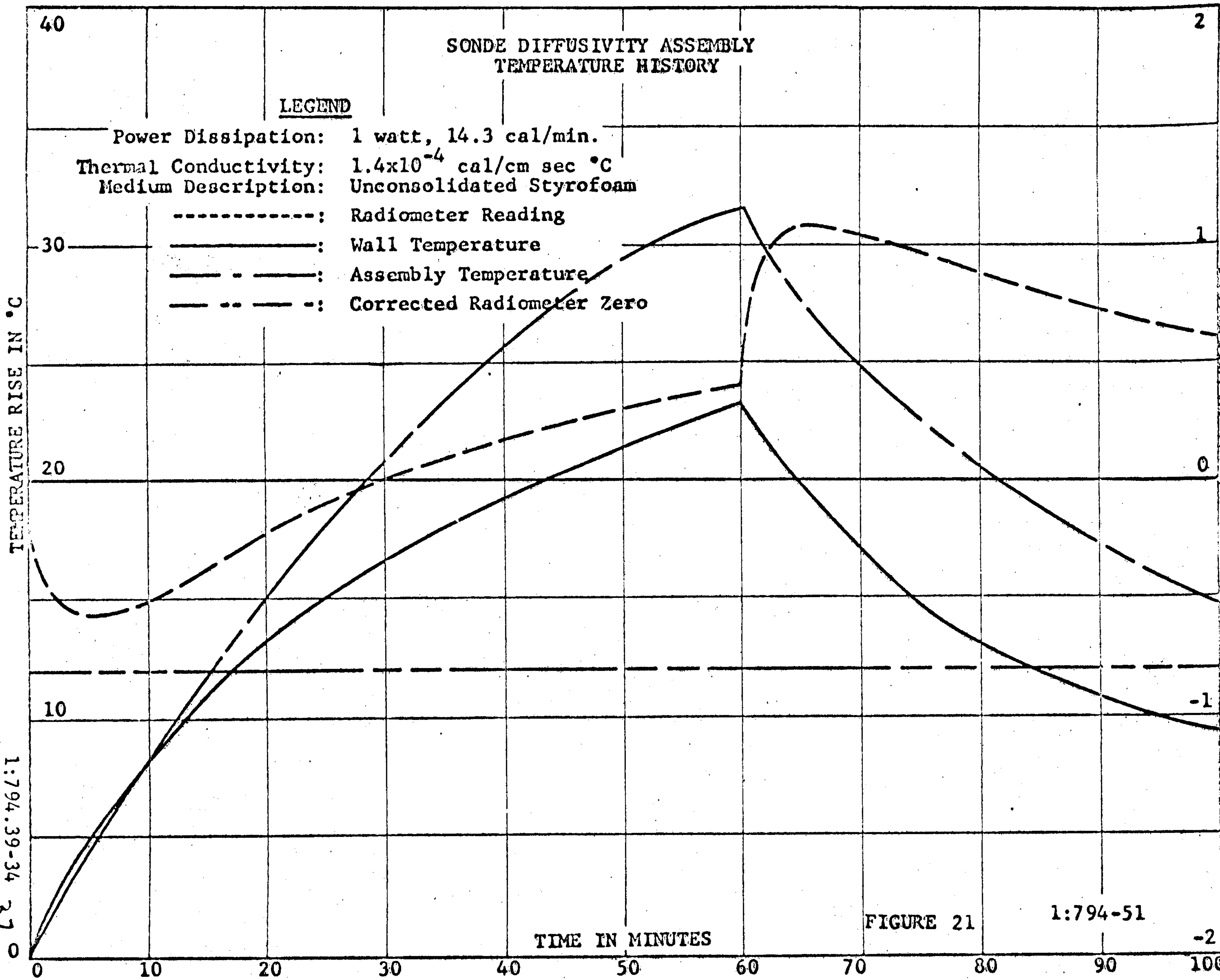

FIGURE 21

RE-ORDER No. 61-563

1:794.39-34
1:794-51

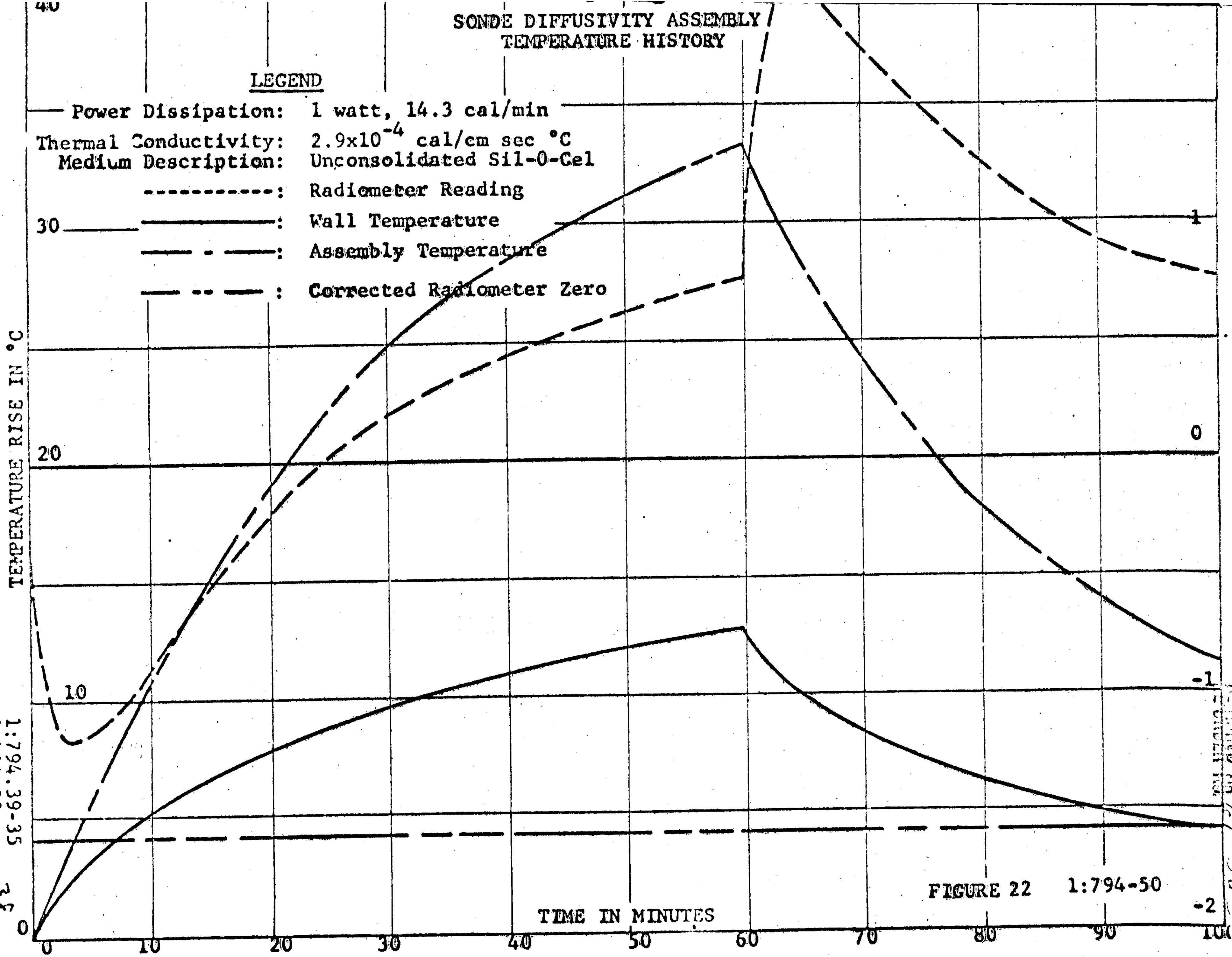

FIGURE 22 1:794-50

1:794.39-35
1:794-50

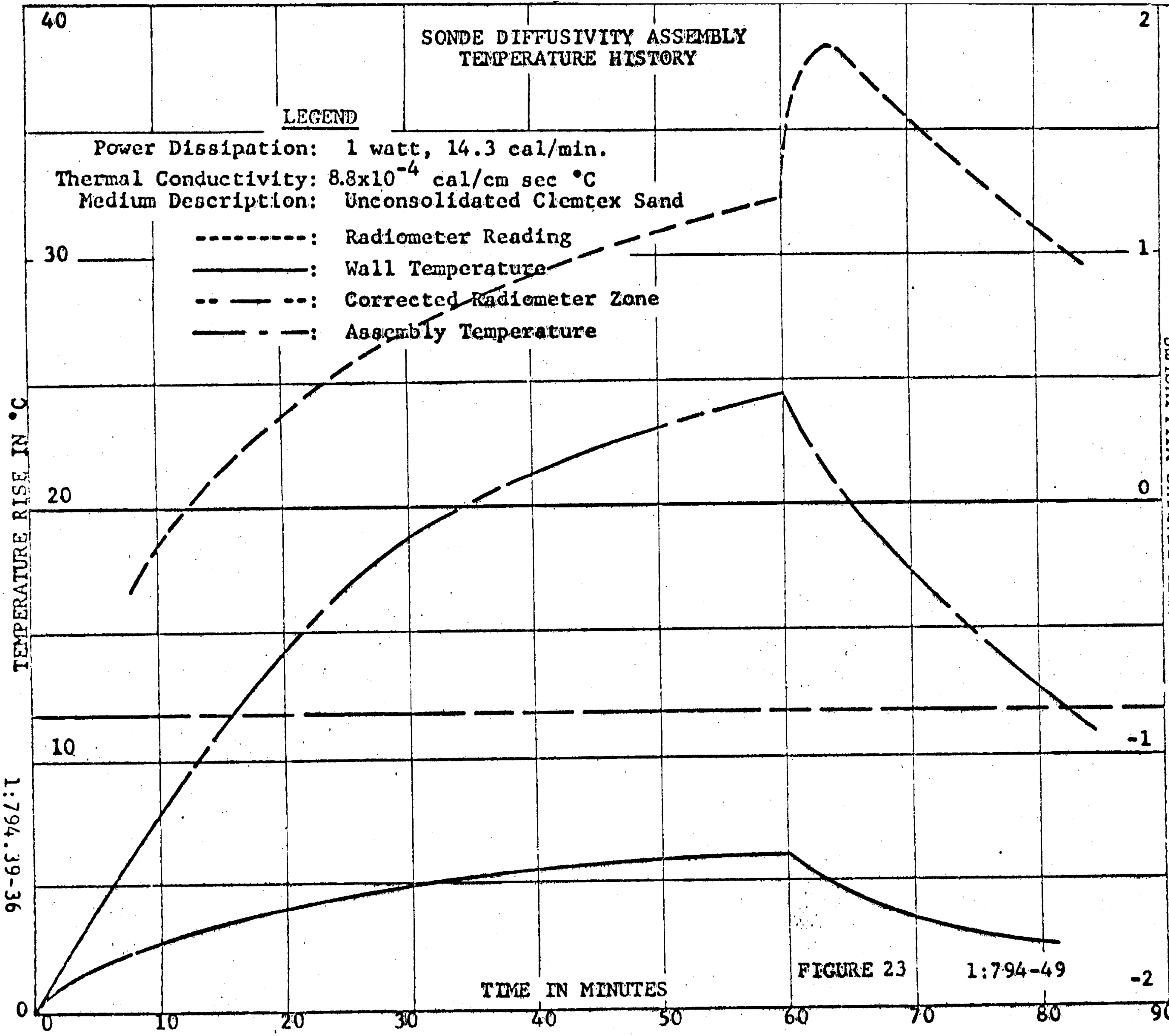

FIGURE 23 1:794-49

1:794.39-36
1:794-49

RE-ORDER No. 61-563

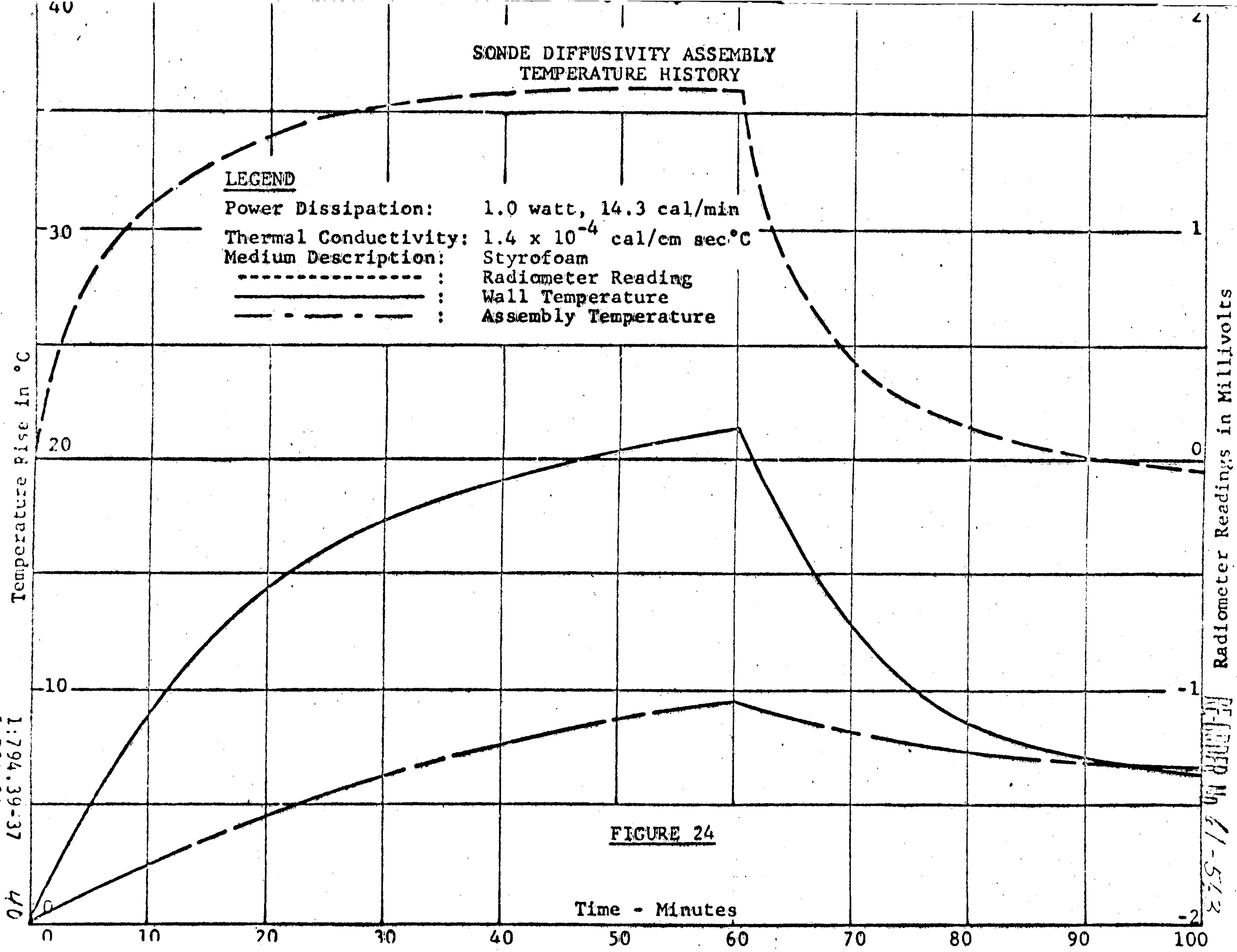

FIGURE 24

1:794.39-37
1.794-96

RE-ORDER No. 61-523

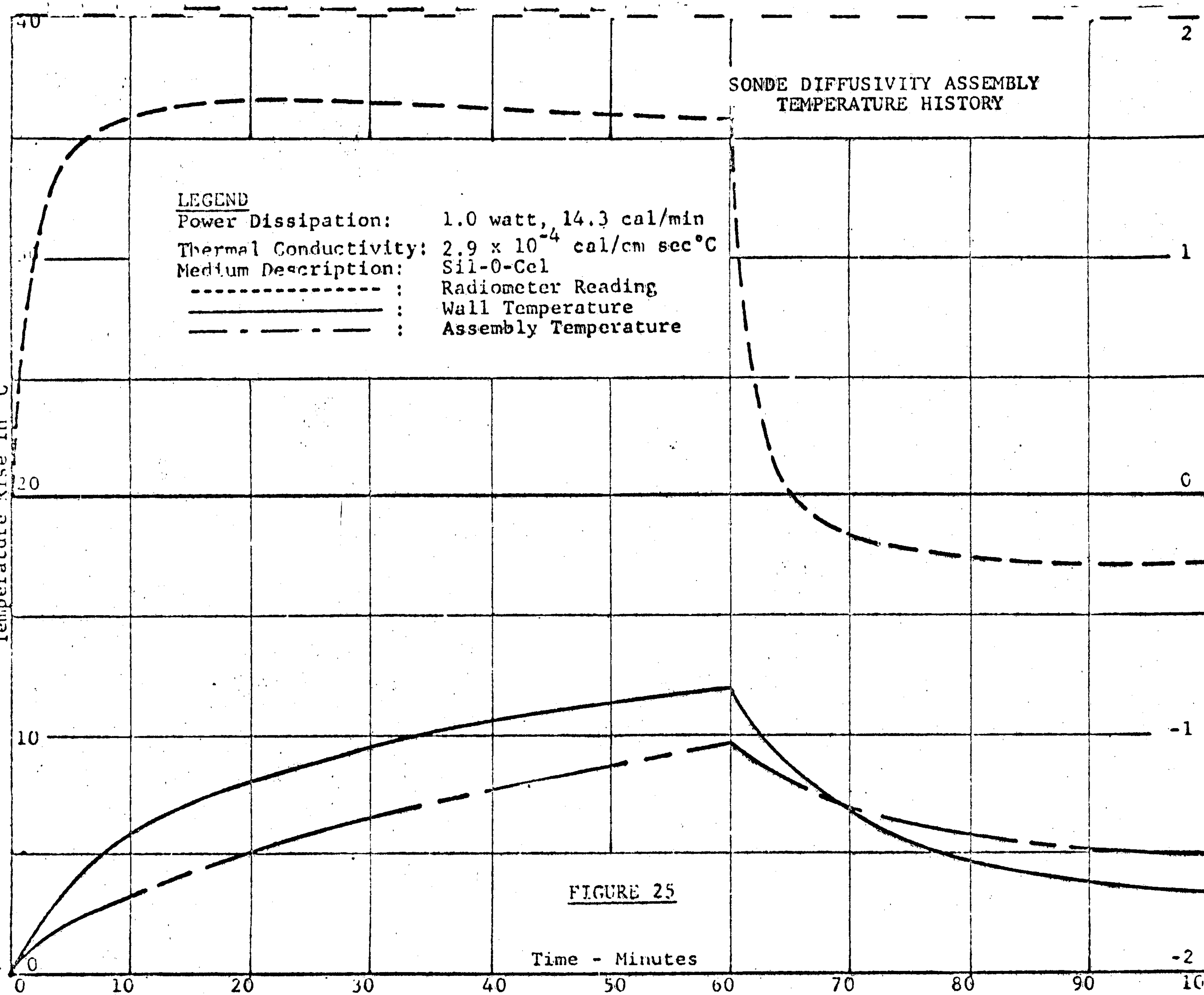

FIGURE 25

RE-ORDER No. 61-563

1:794.39-38
1.794-97

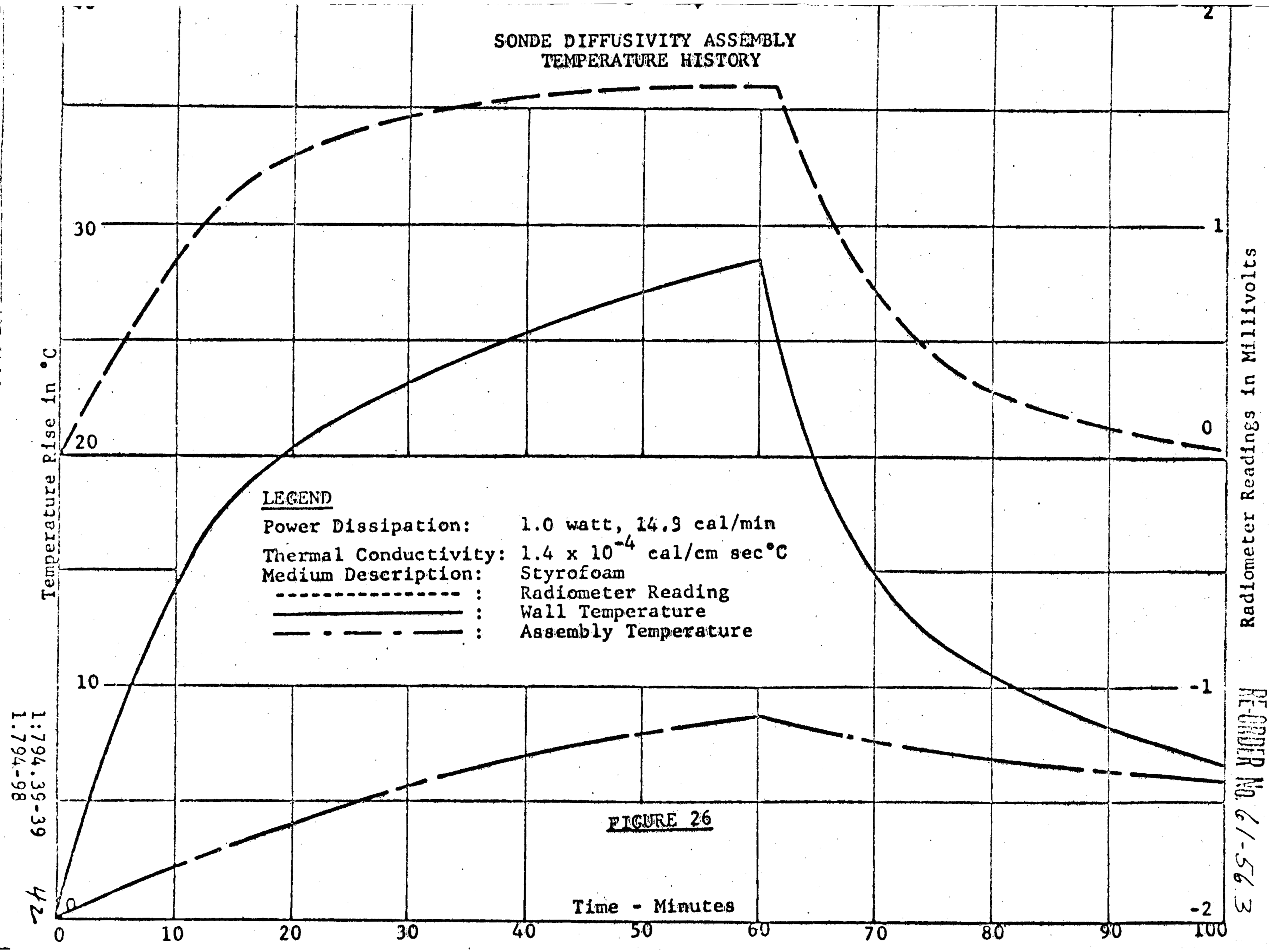

FIGURE 26

RE-ORDER No. 61-563

1:794.39-39
1.794-98

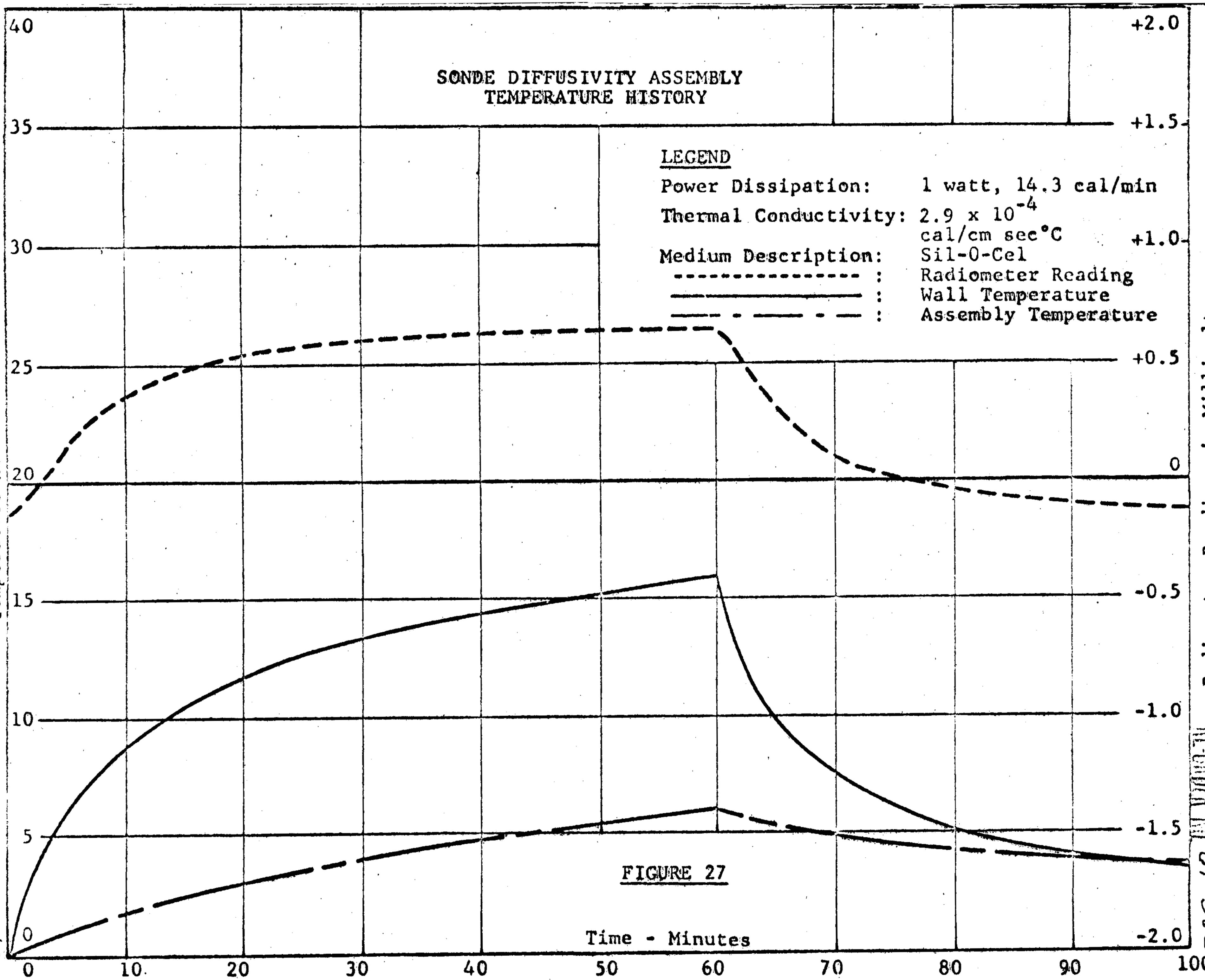

FIGURE 27

1:794.39-40
1.794-99

RE-ORDER No. 61-563